Trend Analysis of the North America Wildfires Using MAIAC MODIS Record

Alexei Lyapustin, NASA GSFC
Amanda Wang (River Hill High School, MD)
Yujie Wang (UMBC)

Sergey Korkin (UMBC), Sujung Go (UMBC),
Myungje Choi (UMBC)

Sun-Climate Symposium
Flagstaff, Arizona, October 16-20, 2023

Forest Wildfires - Overview

From IPCC AR6

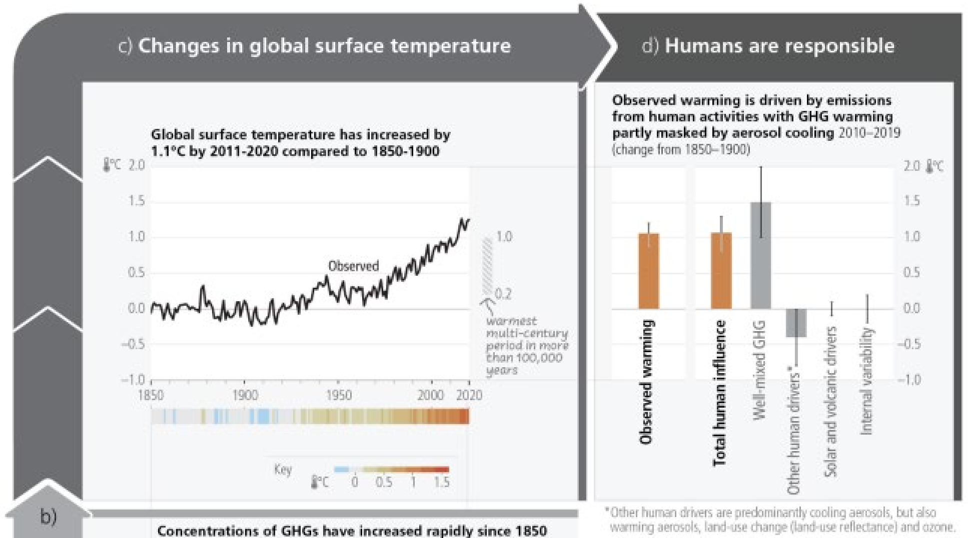
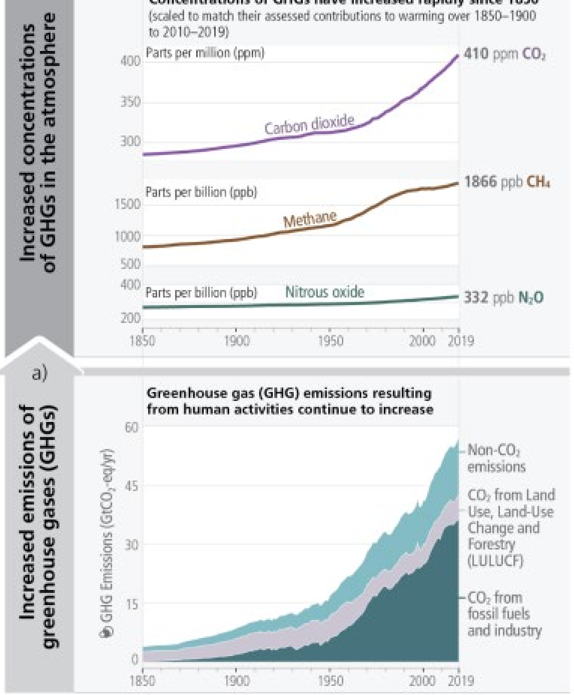

Vapor Pressure Deficit (VPD)

$$VPD = P_s - P$$

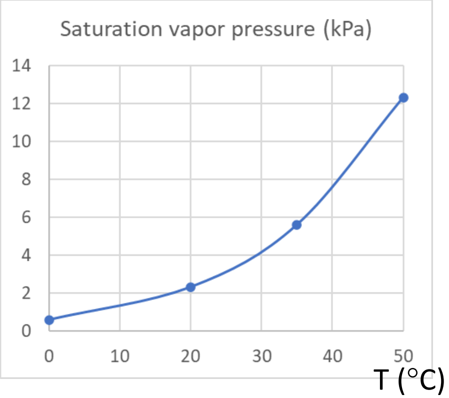

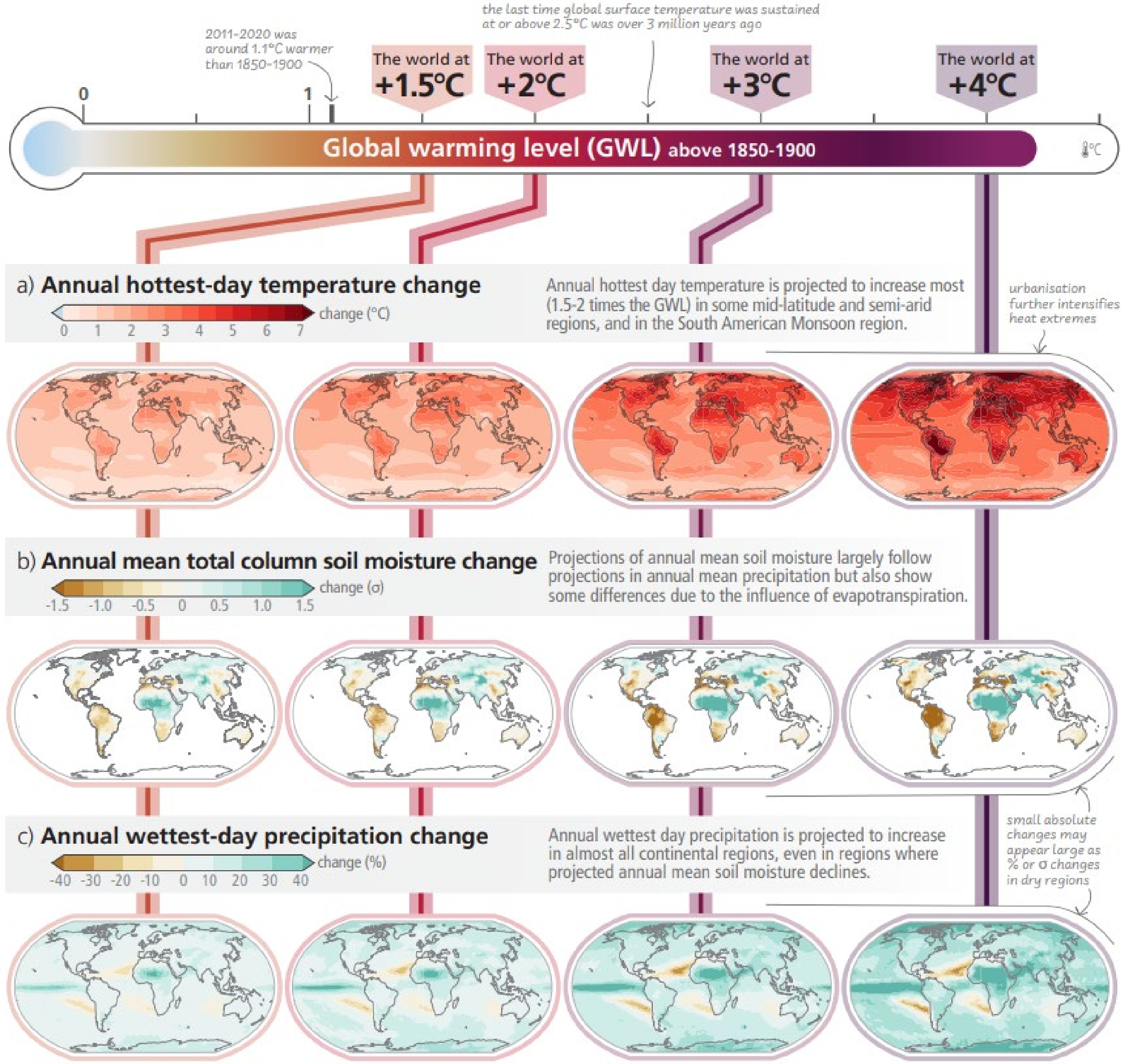

Figure SPM.2: Projected changes of annual maximum daily maximum temperature, annual mean total column soil moisture and annual maximum 1-day precipitation at global warming levels of 1.5°C, 2°C, 3°C, and 4°C relative to 1850–1900. Projected **(a)** annual maximum

H. Clarke et al., Forest fire threatens global carbon sinks and population centres under rising atmospheric water demand, Nature Comm. (2022) 13:7161, https://doi.org/10.1038/s41467-022-34966-3

Vapor pressure deficit (VPD), calculated from air temperature and humidity, is a direct measure of the atmospheric demand for water. It is a reliable predictor of dead fuel moisture content, and a key driver of plant mortality, causing declines in the moisture content of live fuels. The comfortable VPD range for vegetation is 0.45-1.3 kPa, with median of 0.85 kPa. Here, VPD is calculated based on ERA-5 reanalysis.

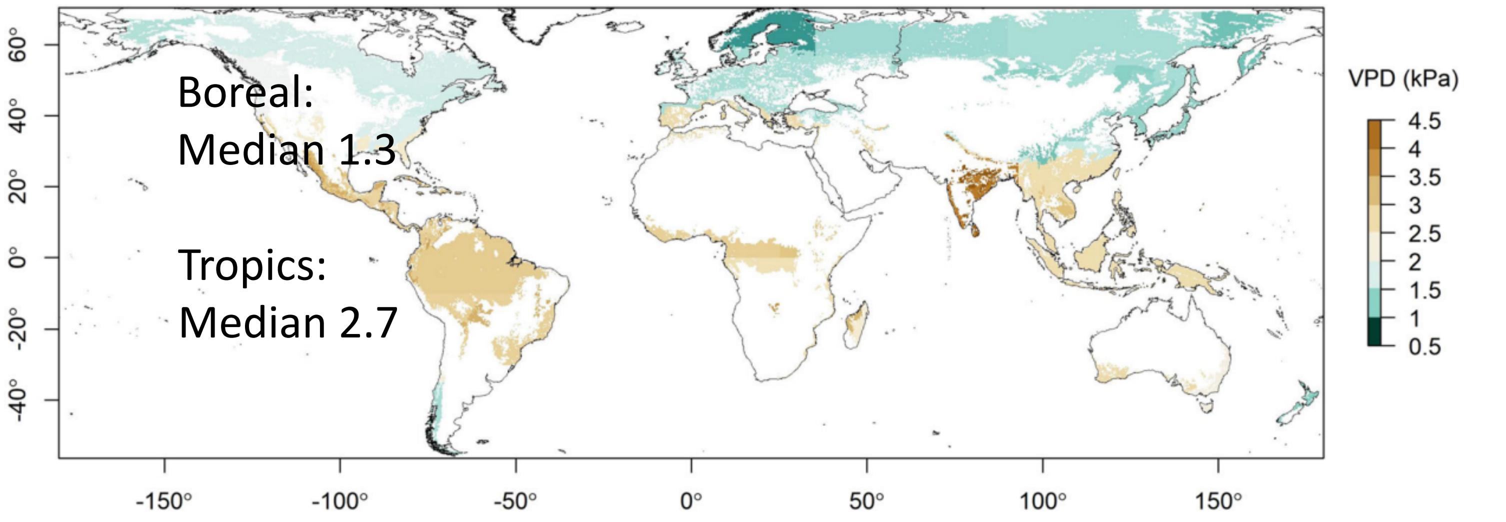

Fig. 2 | VPD thresholds (kPa) for fire activity in global forest biomes. Threshold values indicate the daily VPD above which the probability of fire exceeds 50%, as derived from generalised linear modelling of historical climate and fire records. The white areas indicate non-forest land.

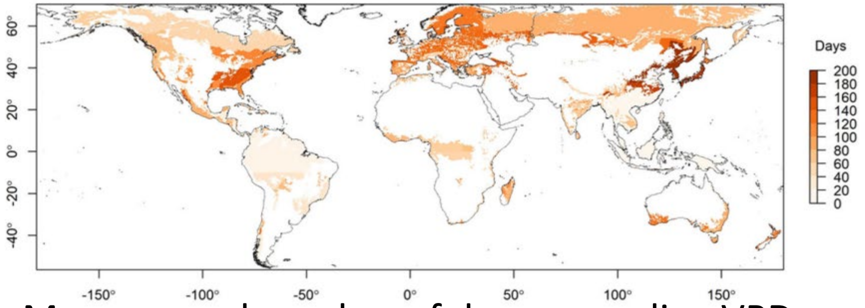

Mean annual number of days exceeding VPD threshold for global forests (ERA5, 2003-2020)

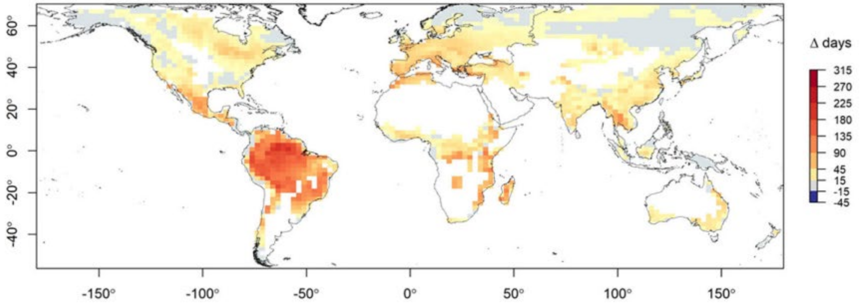

Change in exceedance by 2100 under RCP8.5

Amazon forests may turn from sink to source of carbon.
Human smoke exposure is expected to increase in central America, eastern and western Africa, India, China and south Asia.

Martín Senande-Rivera et al., Spatial and temporal expansion of global wildland fire activity in response to climate change, Nature Comm. (2022) 13:1208 | https://doi.org/10.1038/s41467-022-28835-2

Temperature and precipitation define (vegetation type, density etc. – fuel) fire-prone regions. Analysis based on CMIP5, worst case scenario.

Present

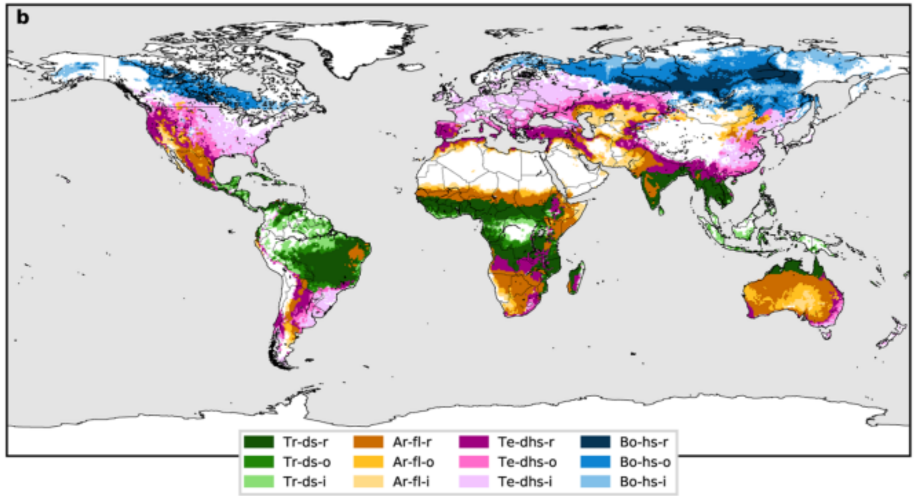

Br – Boreal
Te – Temperate
Ar – Arid
Tr – Tropical

R – recurrent
O – occasional
I - infrequent

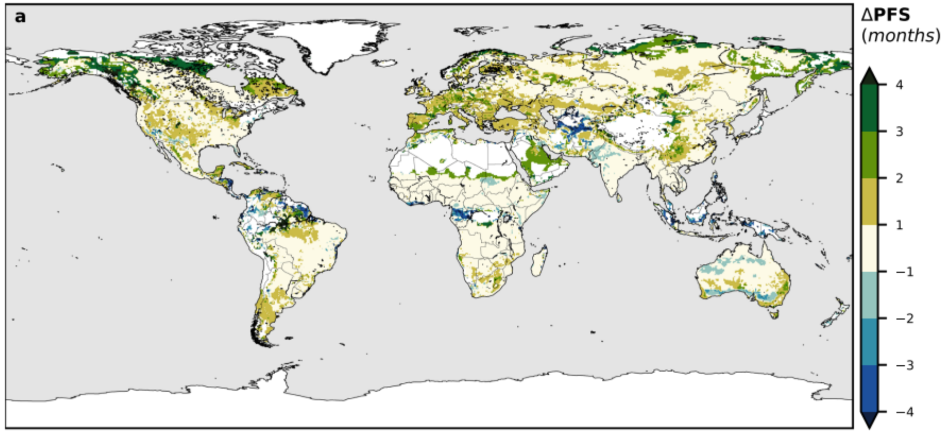

Change in potential fire season length between current and future climate

Future
2070-2099

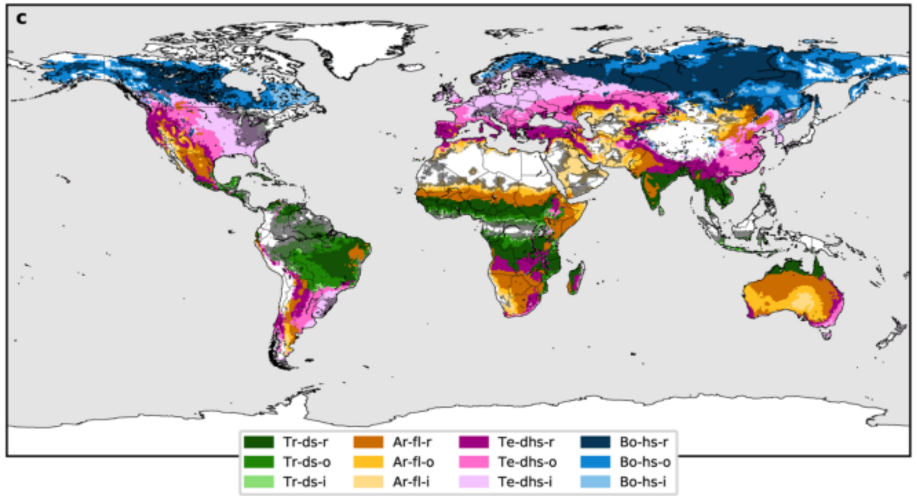

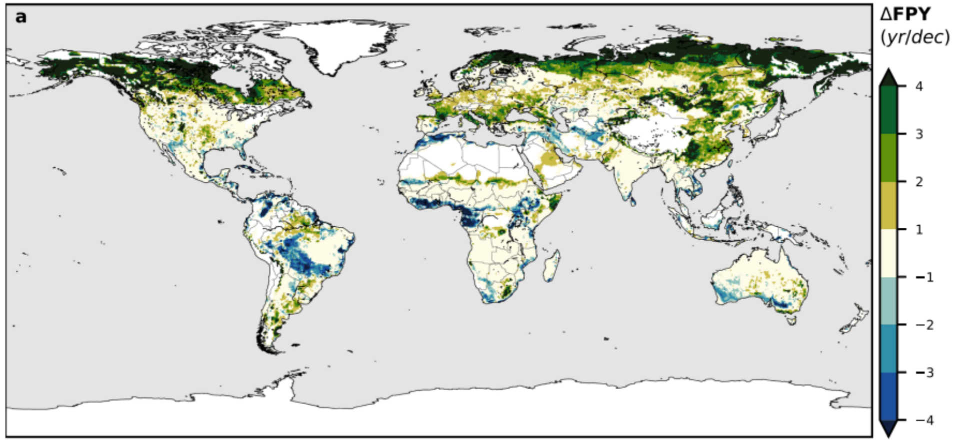

Fig. 2 Fire-prone region classification. a With observed burned area data as a reference: not classified (NC, white) and misclassified (C, black) areas with $BA_{max} = 0$ ha, unclassified (NC, grey) and classified (Tr-ds, Ar-fl, Te-dhs and Bo-hs) areas with $BA_{max} > 0$ ha. Each class is subdivided into three subcategories depending on the recurrence of the fire-prone conditions: recurrent (r), occasional (o) and infrequent (i). **b** Present (1996–2016) fire-prone climatic regions. **c** Future (2070–2099) fire-prone climatic regions with shaded grey representing a <75% confidence percentage, estimated as the percentage of CMIP5 Global Circulation Models (GCMs) agreeing on the result.

Change in potential fire years per decade between current and future climate

J.C. Canadell et al., Multi-decadal increase of forest burned area in Australia is linked to climate change, Nature Comm. | (2021) 12:6921 | https://doi.org/10.1038/s41467-021-27225-4

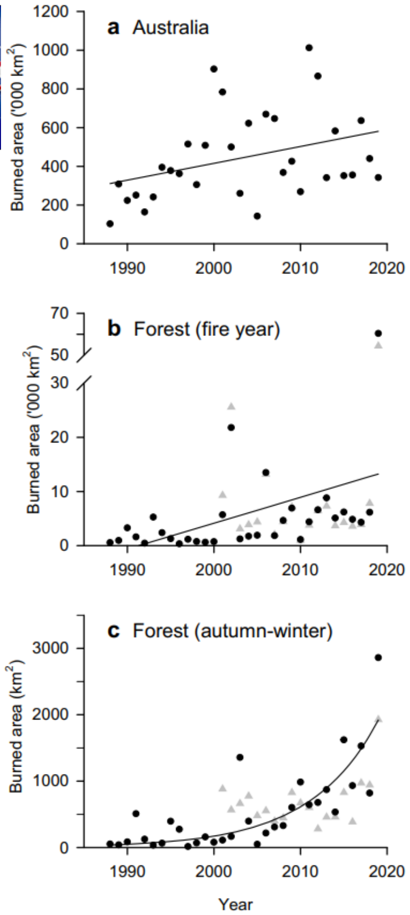

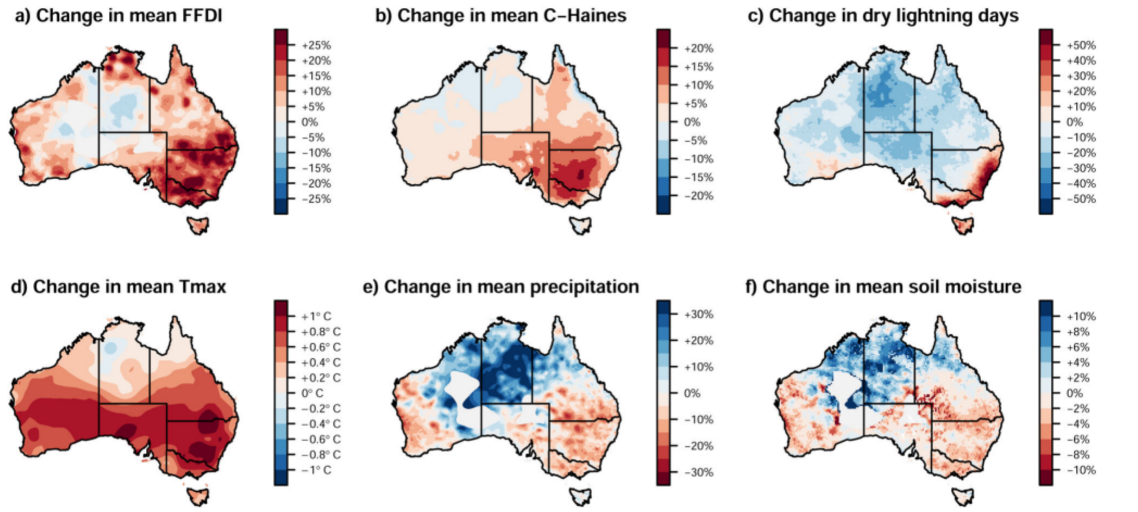

Fig. 5 Climate change factors associated with wildfire weather and activity. a Near-surface fire weather conditions based on the Forest Fire Danger Index, (**b**) mid-tropospheric fire weather conditions based on the C-Haines Index, (**c**) dry lightning conditions as key factors for ignitions, (**d**) daily maximum temperature, (**e**) annual rainfall deficit and (**f**) soil moisture (0–23 cm) associated with dryness of the forest system. Changes are calculated as the changes from 1980–1999 to 2000–2019, calendar years, for all variables except for dry lightning to 2000–2016. Grey areas in (**e**) and (**f**) denote areas with insufficient data availability.

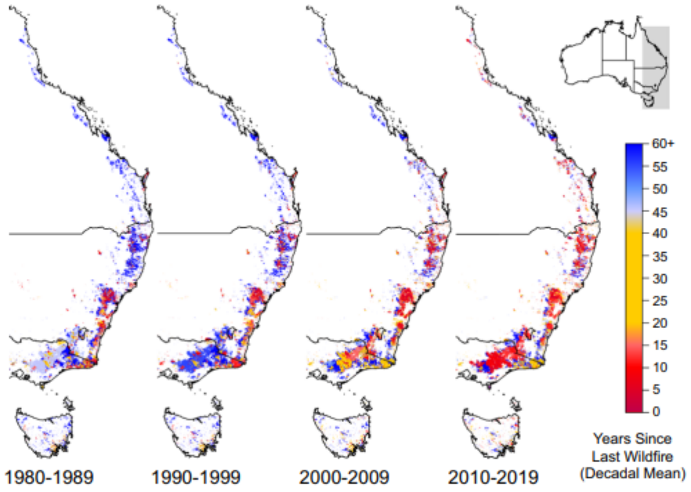

Fig. 4 Number of years since the last wildfire (decadal mean) for forested areas. Analysis based on forested areas that have burned at leas once since fire records began in the 1930s for most states. Spatial resolution is 250-metres. Data: State and Territory fire histories.

Australia's mean temperature has increased by 1.4 °C since 1910 with a rapid increase in extreme heat events, while rainfall has declined in the southern and eastern regions of the continent, particularly during the cool half of the year (This has been associated with a strengthening of the subtropical ridge and a decrease in rainfall from fronts and cyclones).

Burned area in Australia's forests shows:
- a linear positive annual trend;
- an exponential increase during autumn and winter (cold months, reduced precip and drier conditions).
- The mean number of years since the last fire has decreased in each of the past four decades (some ecosystems are in danger, as alpine and mountain ash (forms of eucalyptus, obligate seeders) need 20-30 yrs. for trees to mature and produce seeds)
- The frequency of forest megafire years (>1 Mha burned) has markedly increased since 2000 (2 in 1980-2000 and 9 in 2000-2020).

P. Jain et al., Observed increases in extreme fire weather driven by atmospheric humidity and temperature, Nature Climate Change. (2022) 12, 63-70, https://doi.org/10.1038/s41558-021-01224-1

Analysis of annual extreme values (95th percentile) of fire weather index (FWI), initial spread index (ISI), and VPD based on ERA5 for 1979-2020. FWI and ISI are proxies of fire intensity and spread. Meteofields: air temperature, RH, wind speed (WS) and precip. Results: global mean increase of FWI, ISI, VPD by 14%, 12%, 12%. Decreasing RH is the main driver of >75% changes in FWI and ISI, and T in 40%.

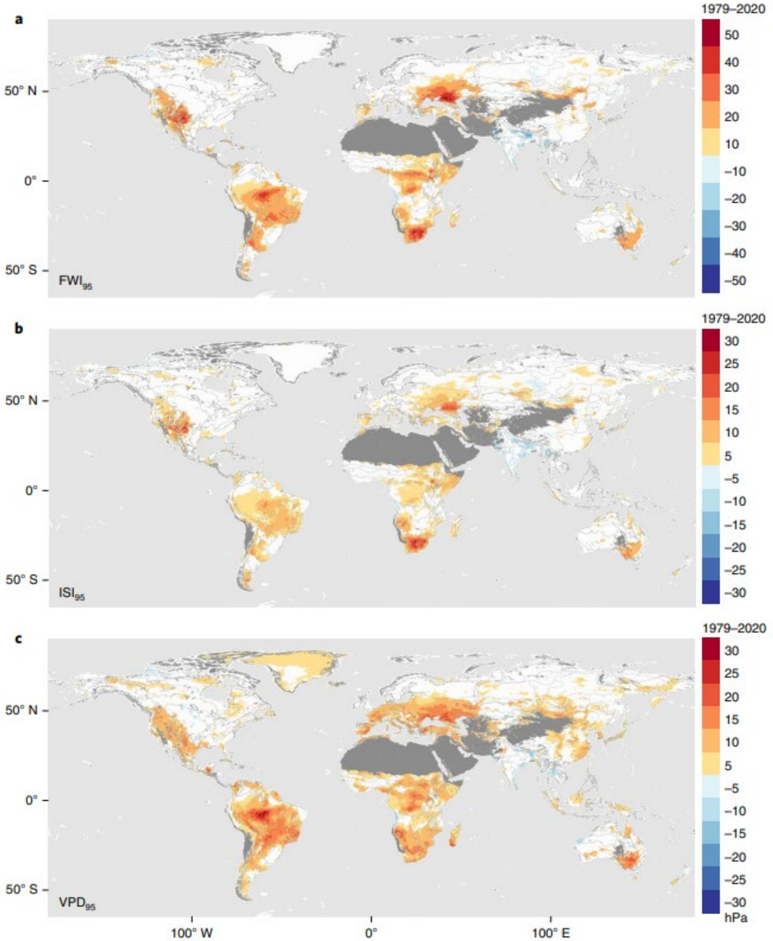

Significant trends in extreme fire weather (1979-2020)

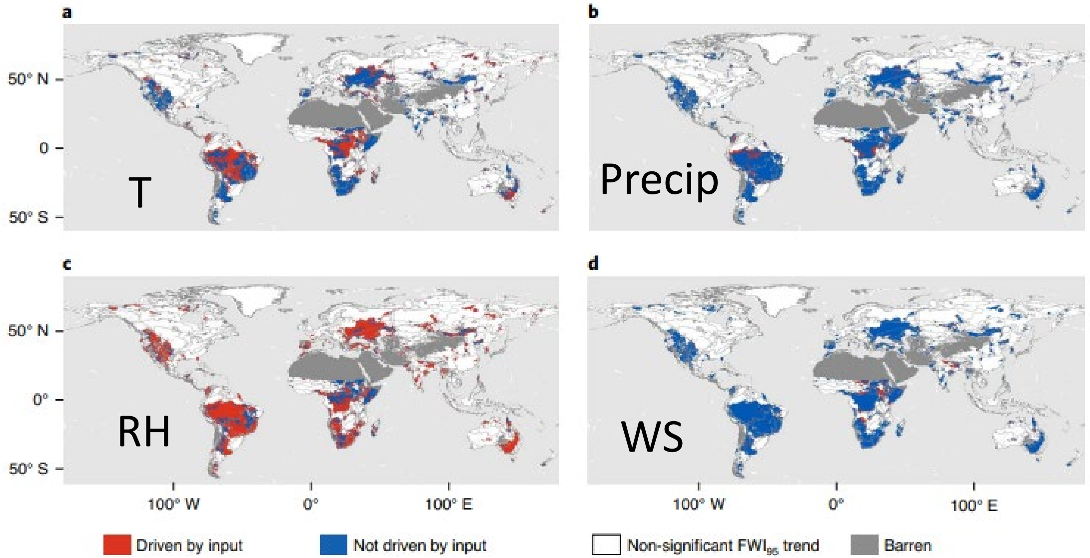

Drivers of extreme fire weather (T, RH, WS at noon; daily Precip.)

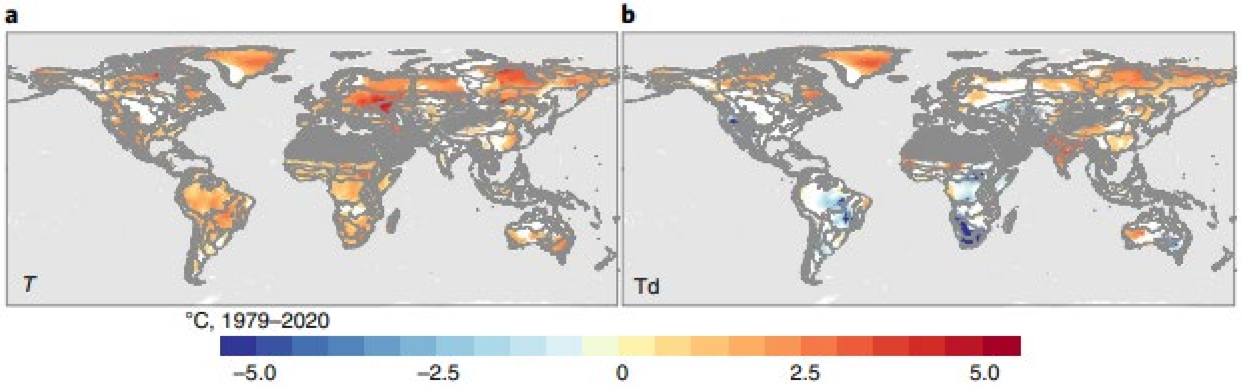

Td – dew point.
Blue – gets drier

Significant trends in mean 2-m T (a) and 2-m Td (b) over the fire season from 1979 to 2020

J.K. Balch et al., Warming weakens the night-time barrier to global fire, Nature (2022) v. 602, 442-448, https://doi.org/10.1038/s41586-021-04325-1

Night-time provides a critical window for slowing or extinguishing fires owing to the lower temperature and lower VPD. If VPD is below threshold (VPD_t) fires naturally extinguish. VPD_t is established based on GOES data as <5% fire detection probability.

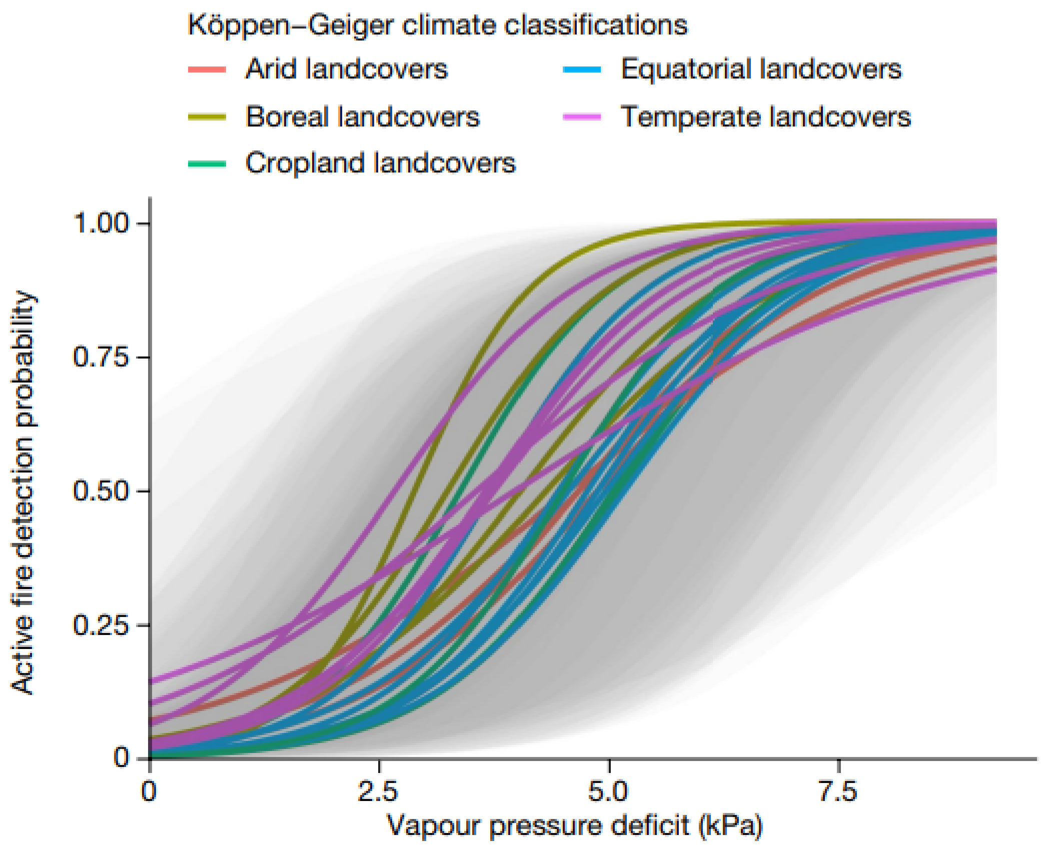

Fig. 2 | VPD provides a key metric for the atmospheric moisture conditions that can cause fire extinction. Predicted relationships between hourly VPD[38] and GOES active fire detections[19] during the burning period of 81,809 fire events in North America and South America. The *y*-axis position represents the

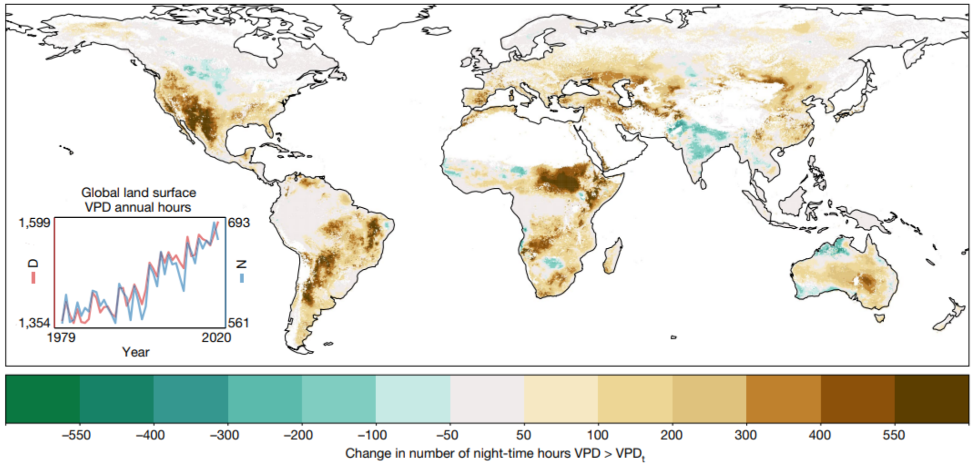

The annual number of flammable night-time hours when $VPD>VPD_t$ increased by over a third from 1979 to 2020.

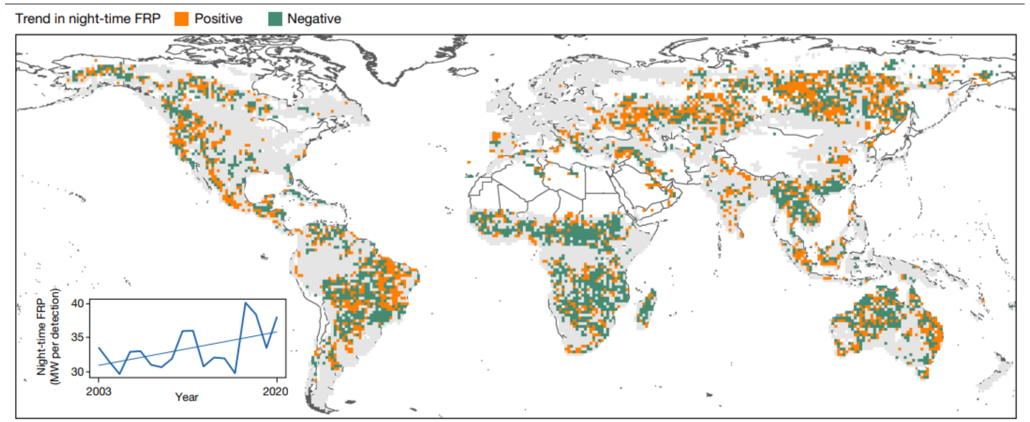

Night-time FRP increased by 7.2% from 2003 to 2020 (based on MODIS).

MAIAC MODIS C6.1

(*Multi-Angle Implementation of Atmospheric Correction*)

Status

MAIAC MODIS C6 available since 2018

MAIAC MODIS C6.1 available since August 2023:

- New regional aerosol models (removes low AOD bias)
- Improved over-ocean algorithm (case I, II waters);
- New alg. over high-sediment (brown) waters;
- Added 0.05° (CMG) operational daily product;
- Developed and implemented a new ***mRTLS*** BRDF model correcting instability at high zenith angles (SZA, VZA > 60°)

MAIAC MODIS Products (Global Sin. Projection)

Atmospheric:

- Cloud/Shadow/Snow Mask,
- CWV (land)
- AOD, FMF (over water),
- Smoke Plume Injection Height (thermal)

Surface:

- BRF (surface reflectance) at 0.5km and 1km;

Surface Daily Gap-Filled:

- 250m Red & NIR NBAR (nadir and local sun at 1:30pm)
- BRDF;
- NDVI (1km);
- Snow grain size and snow fraction (1km);

CMG (0.05°) Daily:

- most of the above + additional VIs

MAIAC MODIS C6.1 Updates

- Developed new regional aerosol models based on AERONET climatology → improves AOD and AC under smoke and dust conditions;

21x21 km^2 (50% coverage), 0.47μm

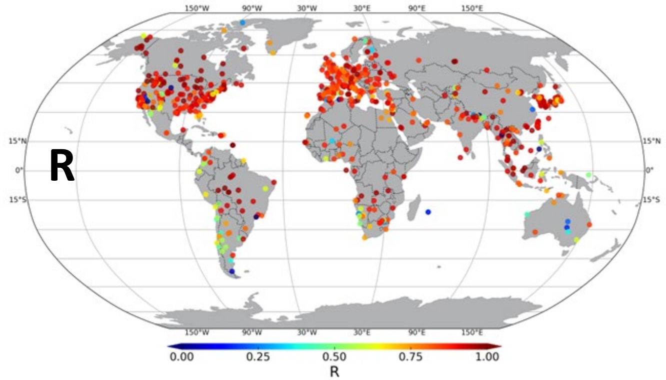

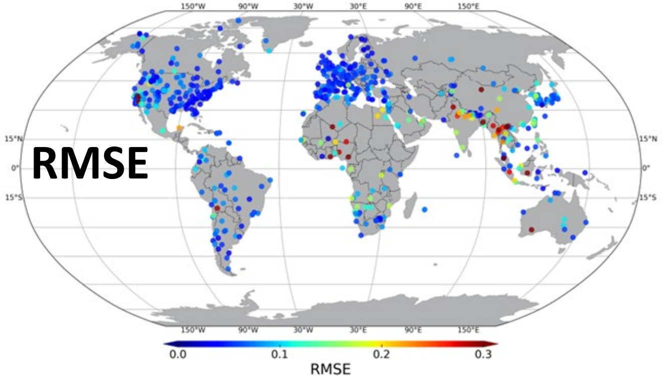

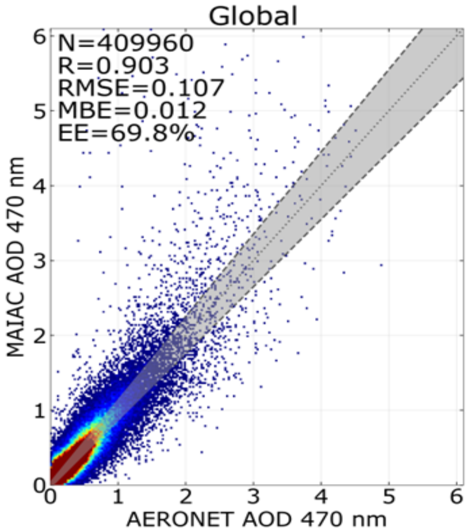

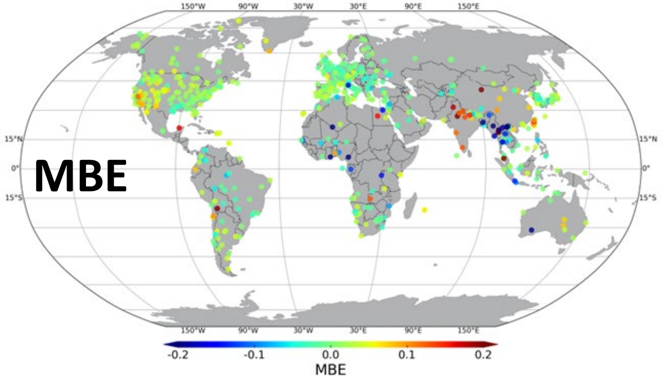

C6 EE $=\pm 0.05 \pm 0.1\tau_{0.47}$

Sept. 2020, Western USA

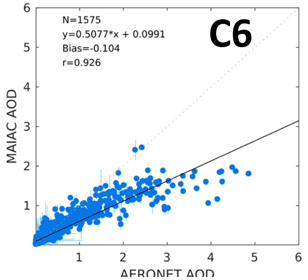

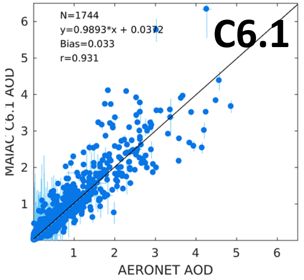

Courtesy: X. Ye, P. Saide (UCLA)

A single 1km pixel

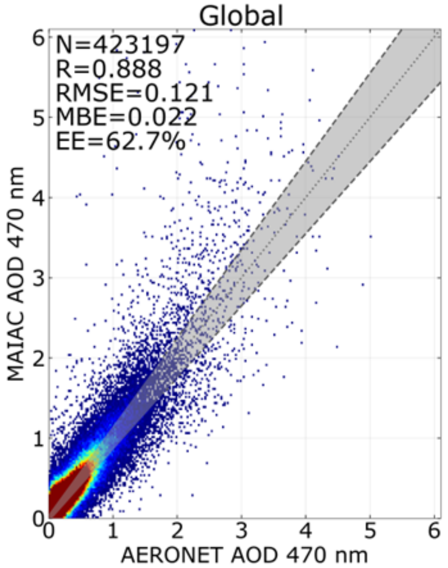

MAIAC	C6	C6.1	C6.1 1km
N	304553	409960	423197
%EE	66%	69.8%	62.7%
R	0.84 →	0.903	0.888
RMSE	0.12 →	0.107	0.121
MBE	0.01	0.012	0.022

Surface Reflectance and Snow

Feb. 17, 2023

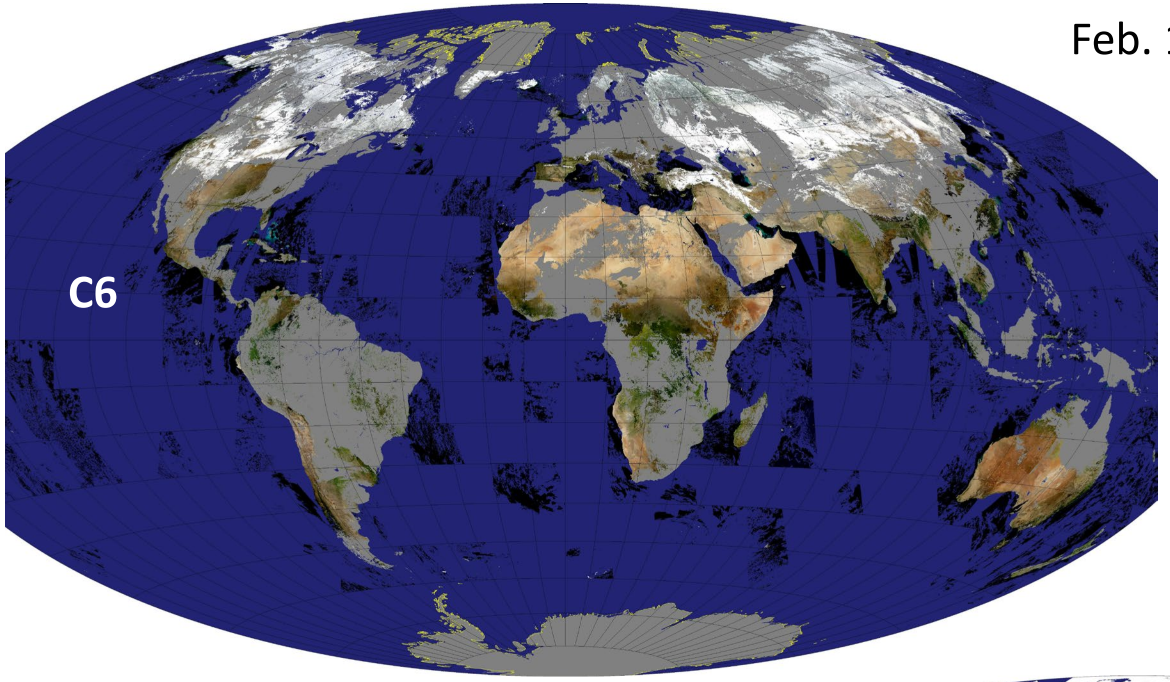

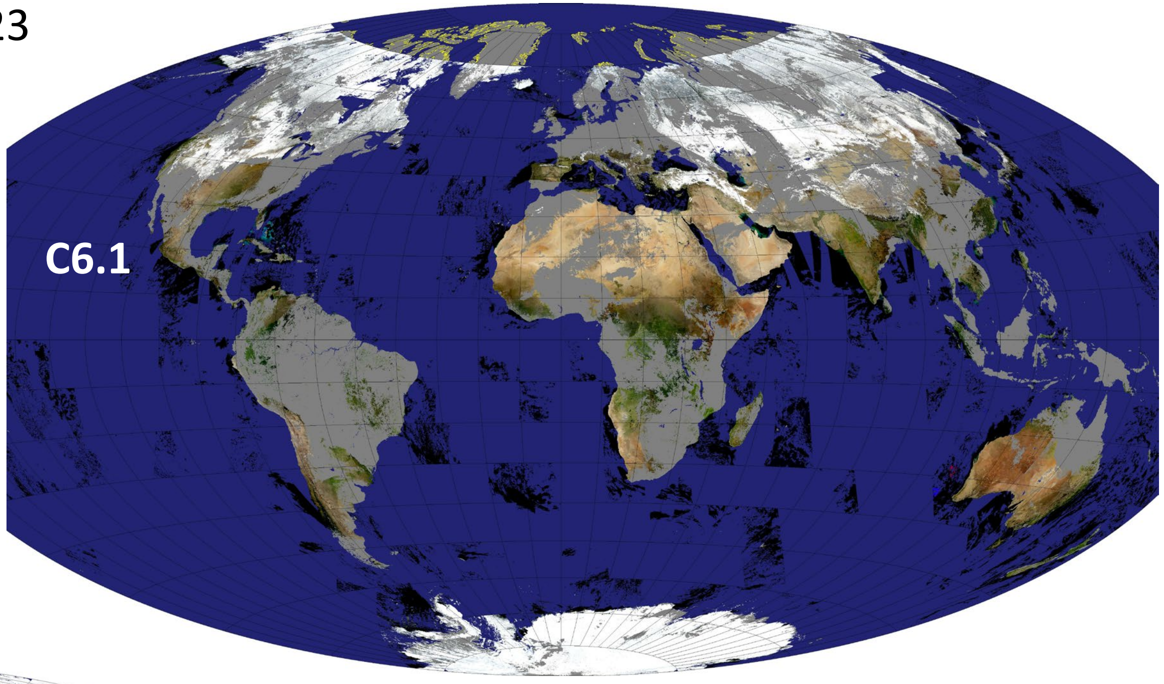

C6.1: May 5, 2023

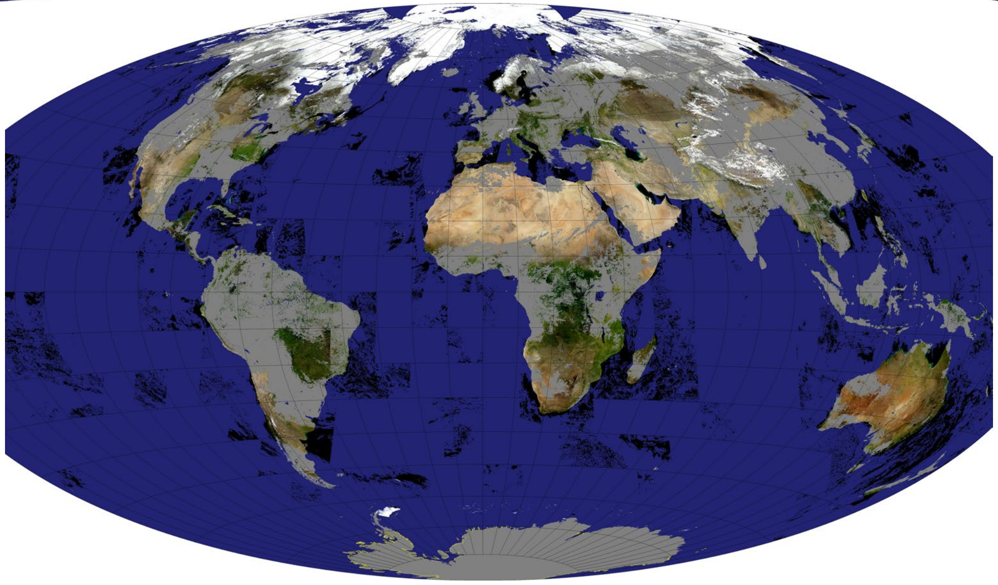

- Improved Snow detection
- Raised SZA_{max} 80°→85°

Surface BRDF: MAIAC vs MCD43

RGB Isotropic Parameter
Sept. 22, 2015

MCD19A3

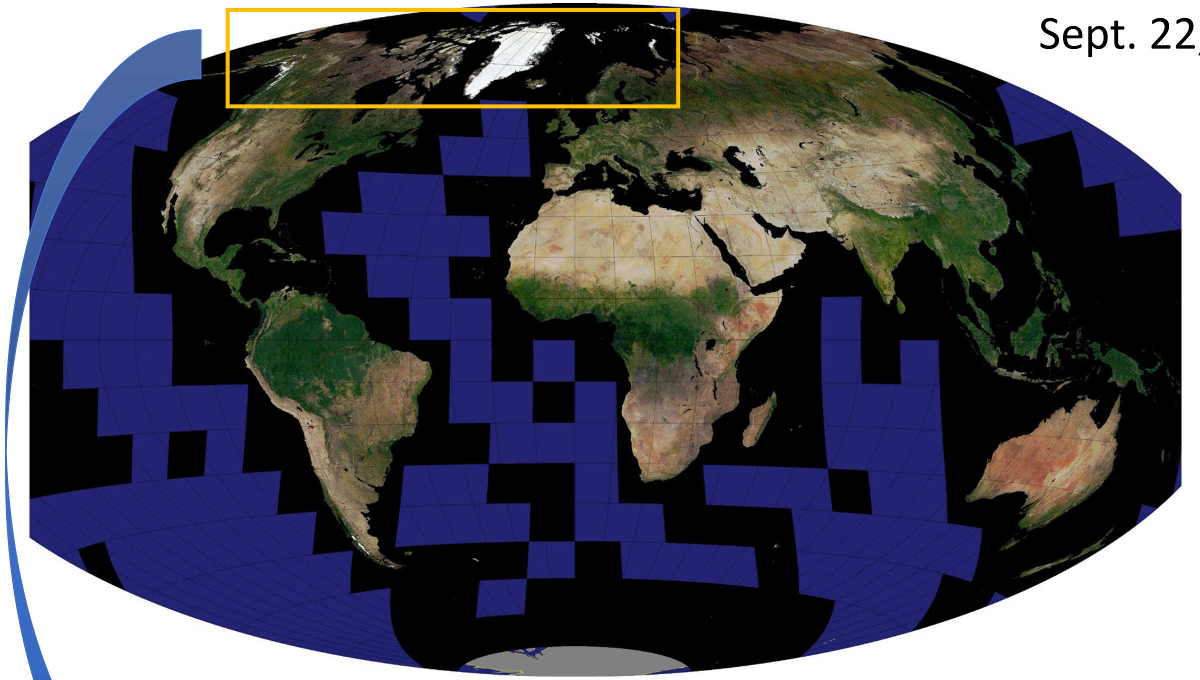

MCD43

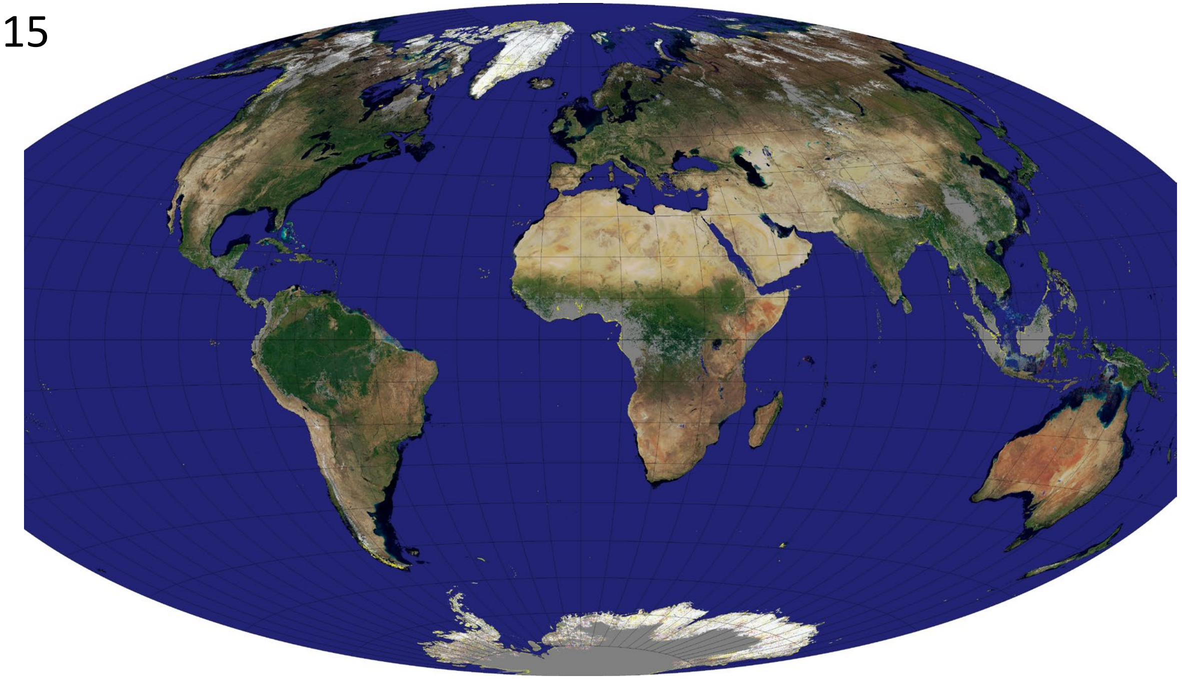

BRDF Over Permanent Snow

MCD19A3

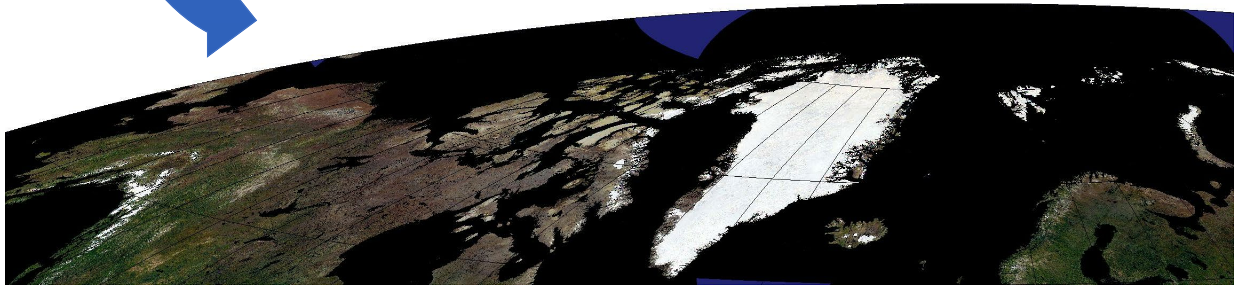

MCD43

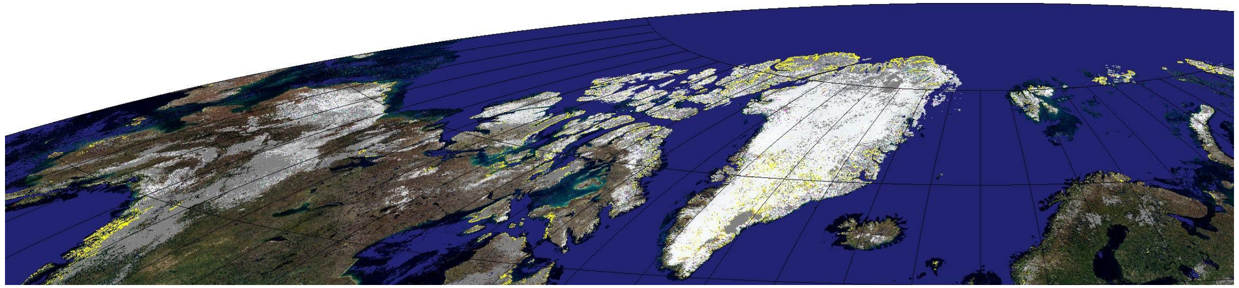

MAIAC Gap-filled NDVI

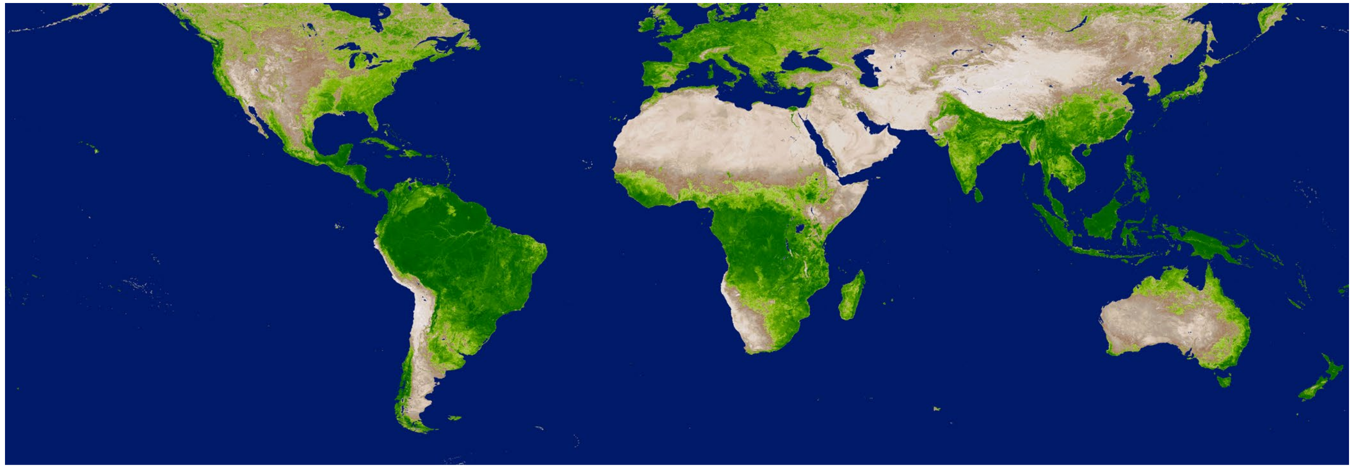

Jan. 17, 2023

July 20, 2022

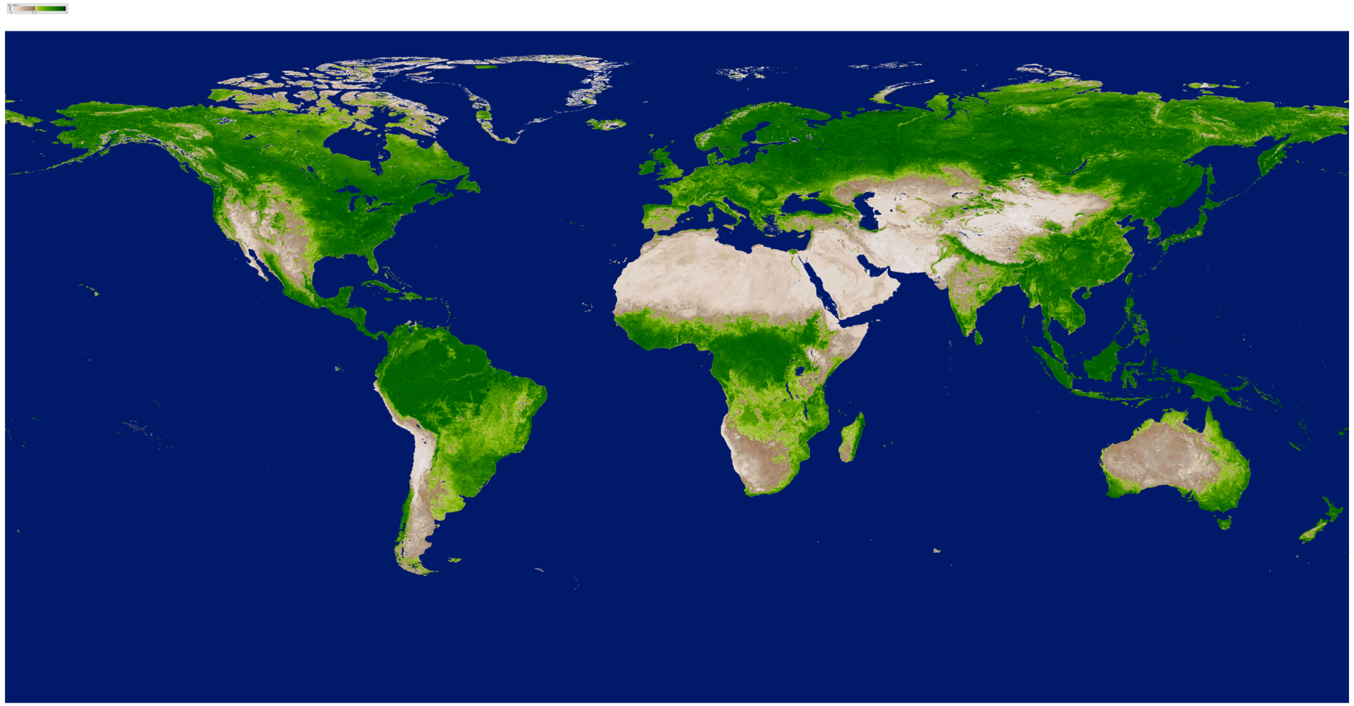

Terra/Aqua MODIS Vegetation Index From MAIAC, Daily L3 CMG SDS:NDVI_gapfill 061
Start Sensor Acquisition Date:
Collection 2022201
Browse image created on Jan 18 13:09:06 2023 UTC, LDOPE

GOALS OF INVESTIGATION

- ❖ **Datasets** (Feb. 2000 – Sept. 2023):
  - MAIAC MODIS AOD, detected HotSpots, CWV, SnowFrac;
  - MERRA-2: Near-surface Temperature (2 m), Precipitation.

- ❖ **Analyze trend of wildfires** manifested in the number of detected hotspots and high aerosol optical depth ($AOD_{0.55}$>1) events across North America using 23+ years of MAIAC MODIS AOD data.

- ❖ **Analyze behavior of confounding factors** including CWV, SnowFrac, T, Precip.

- ❖ **Counting high AOD pixels and fire hotspots**:
  - Calculate daily fractions of 1km land pixels with AOD>1 at $1\times1^{\circ}$ resolution;
  - Aggregate daily data to monthly scale and divide by the number of days in a month
- ❖ **All other data**:
  Compute monthly averages at $1\times1^{\circ}$ resolution

MAY

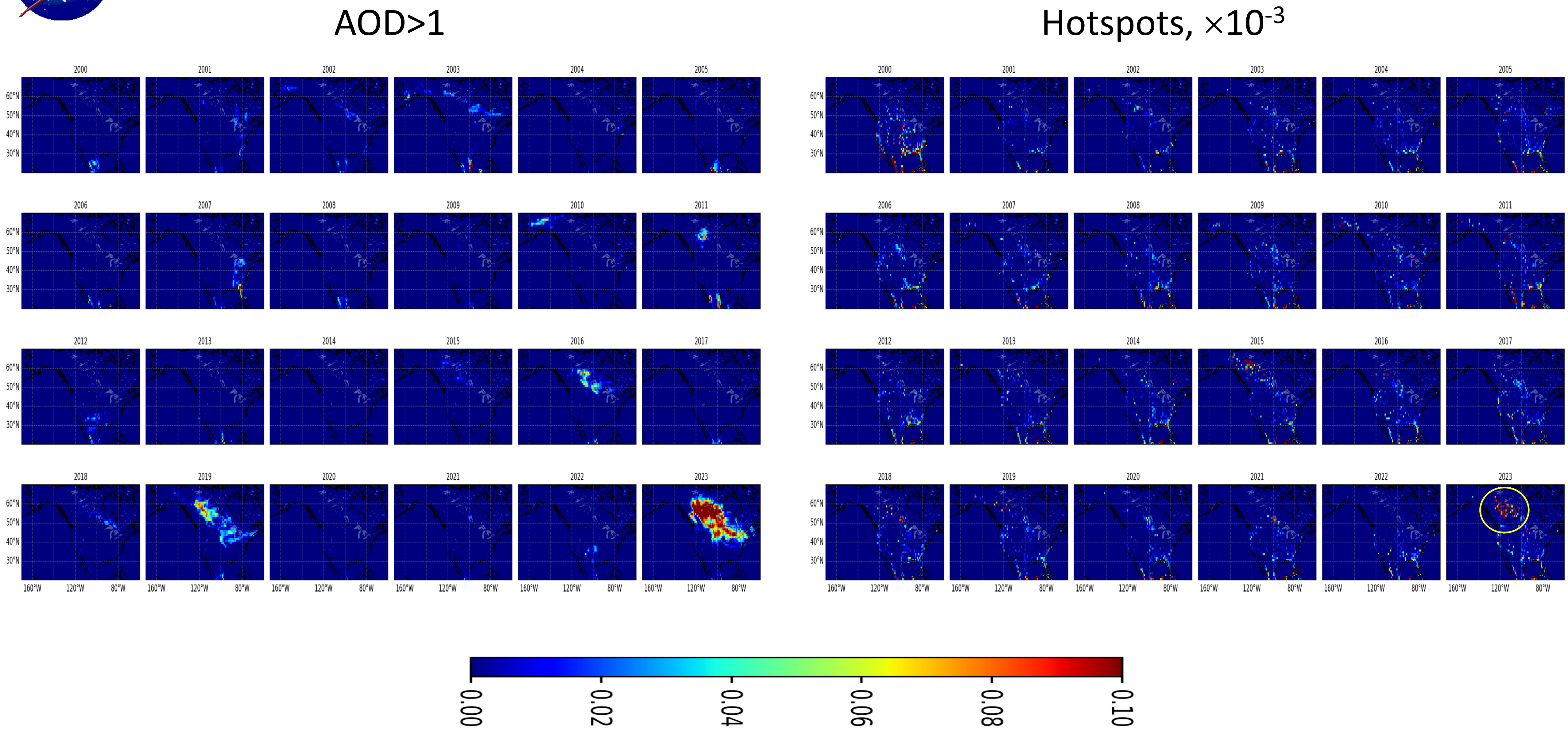

AOD>1
Hotspots, ×10-3
2000
2001
2002
2003
2004
2005
2006
2007
2008
2009
2010
2011
2012
2013
2014
2015
2016
2017
2018
2019
2020
2021
2022
2023
60°N
50°N
40°N
30°N
160°W
120°W
80°W
0.00
0.02
0.04
0.06
0.08
0.10

JUNE

AOD>1

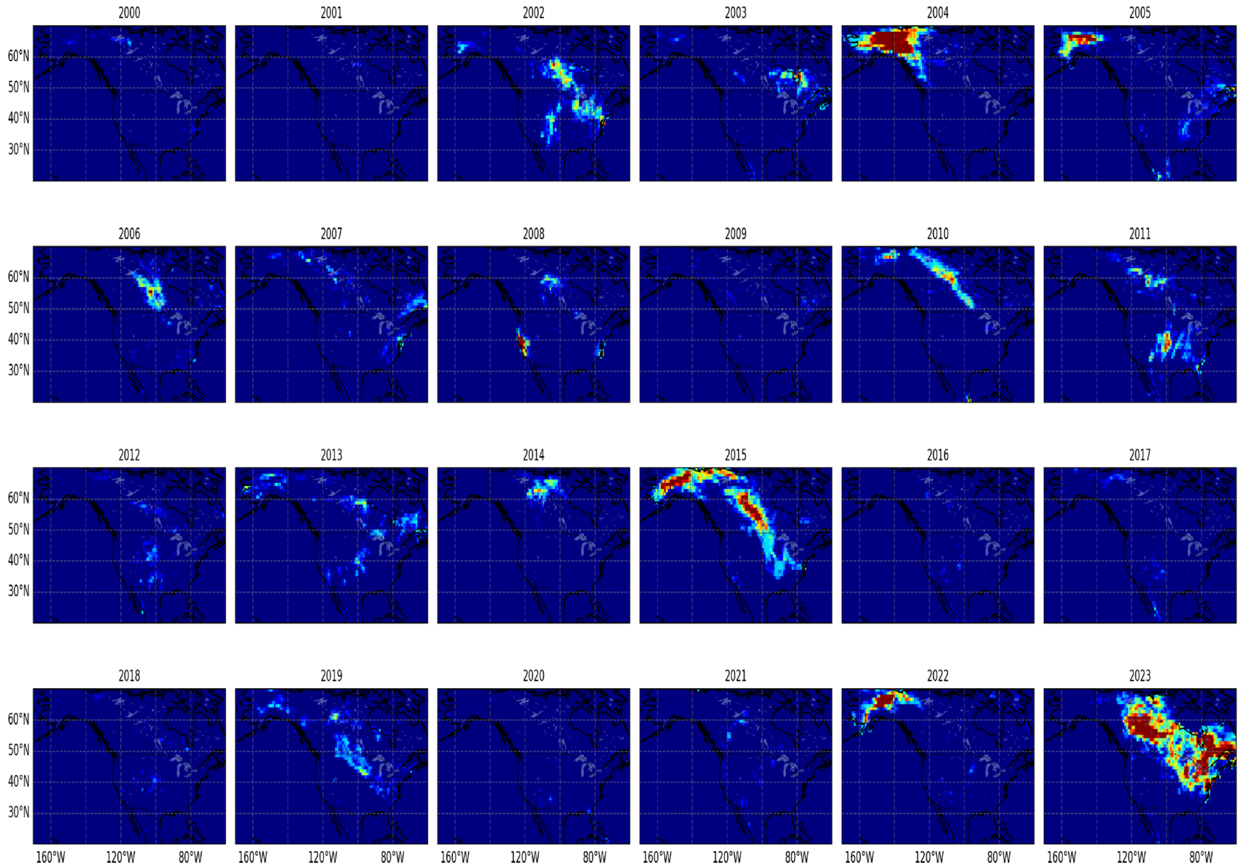

Hotspots, $\times 10^{-3}$

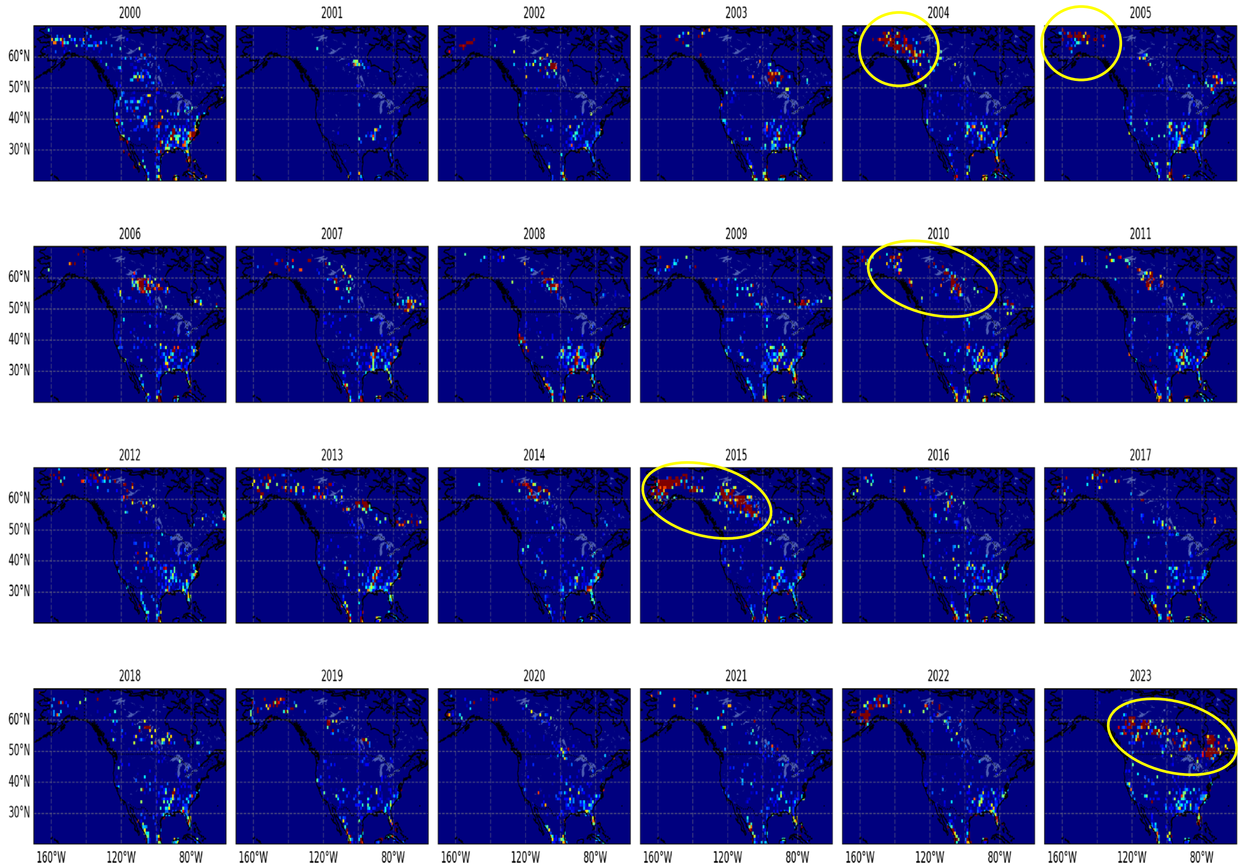

JULY

AOD>1

Hotspots, $\times 10^{-3}$

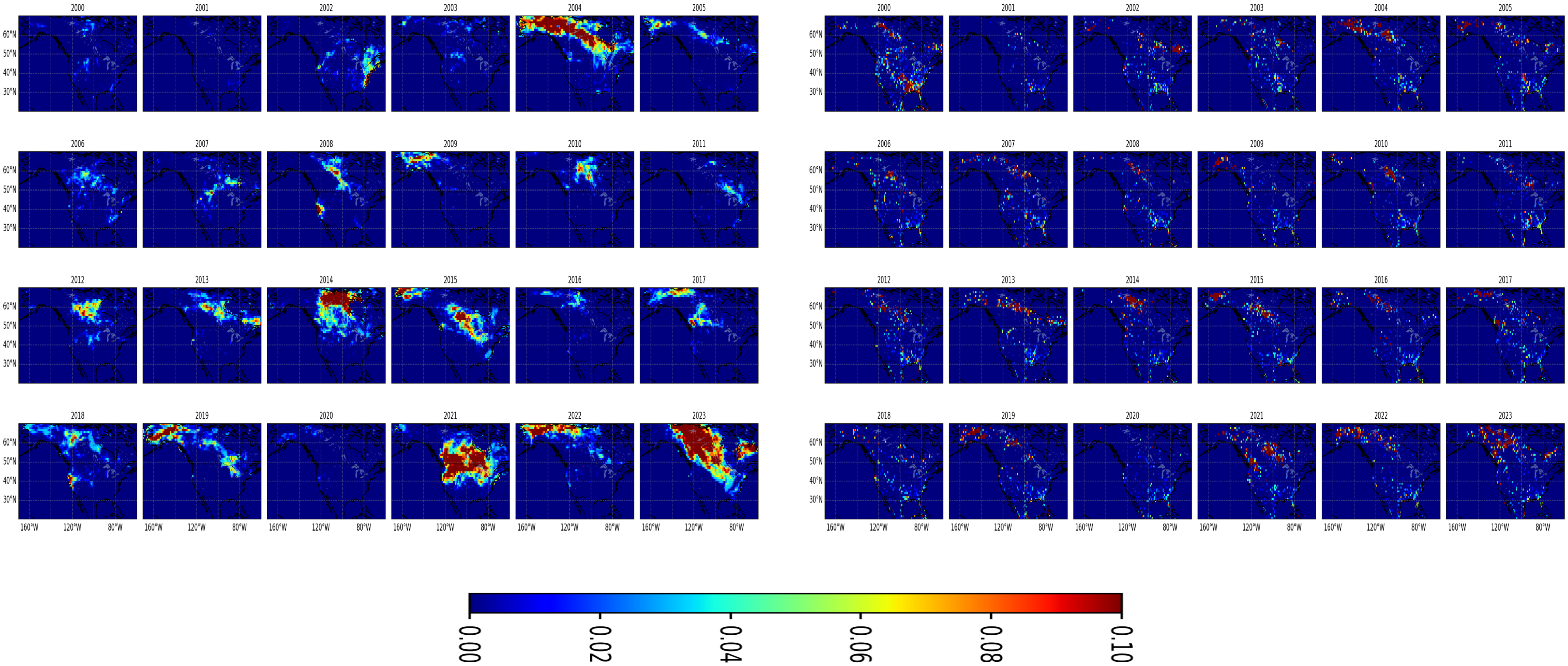

AUGUST

AOD>1

Hotspots, $\times 10^{-3}$

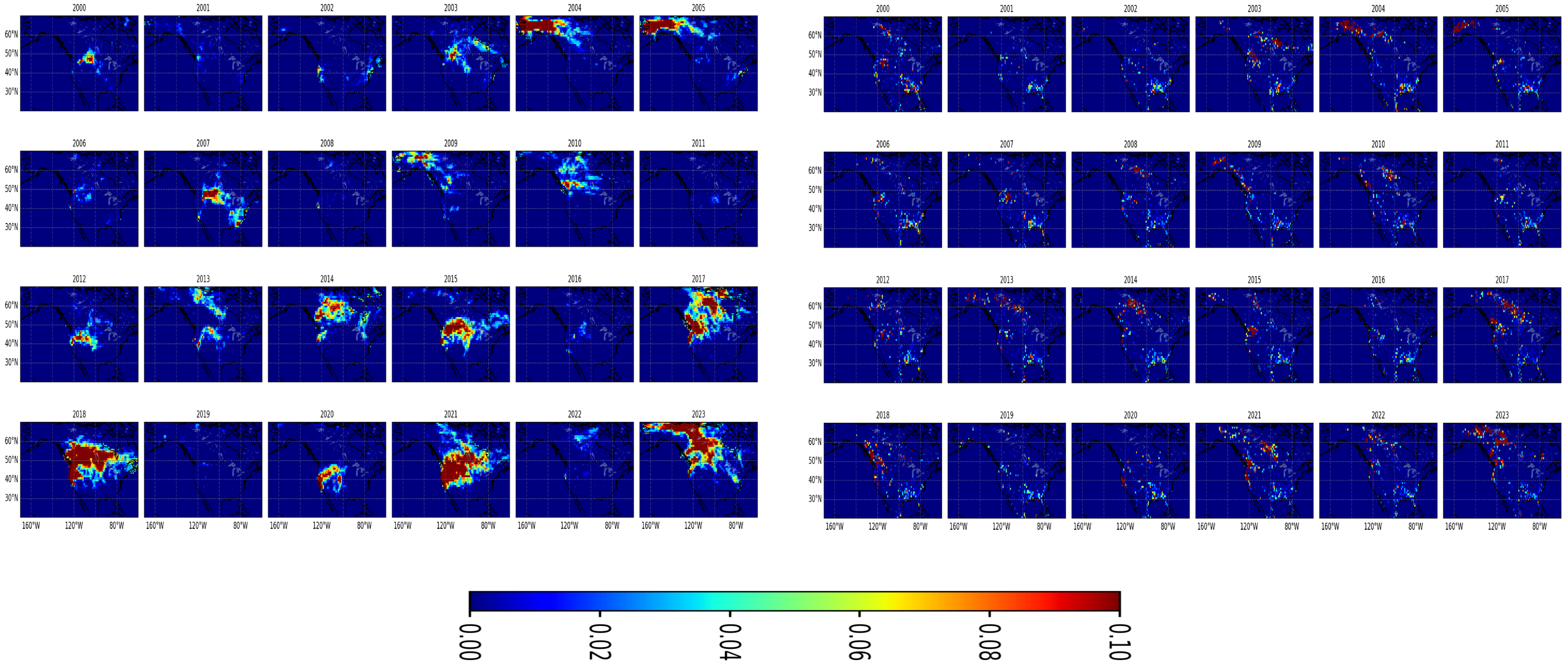

SEPTEMBER

AOD>1

Hotspots, $\times 10^{-3}$

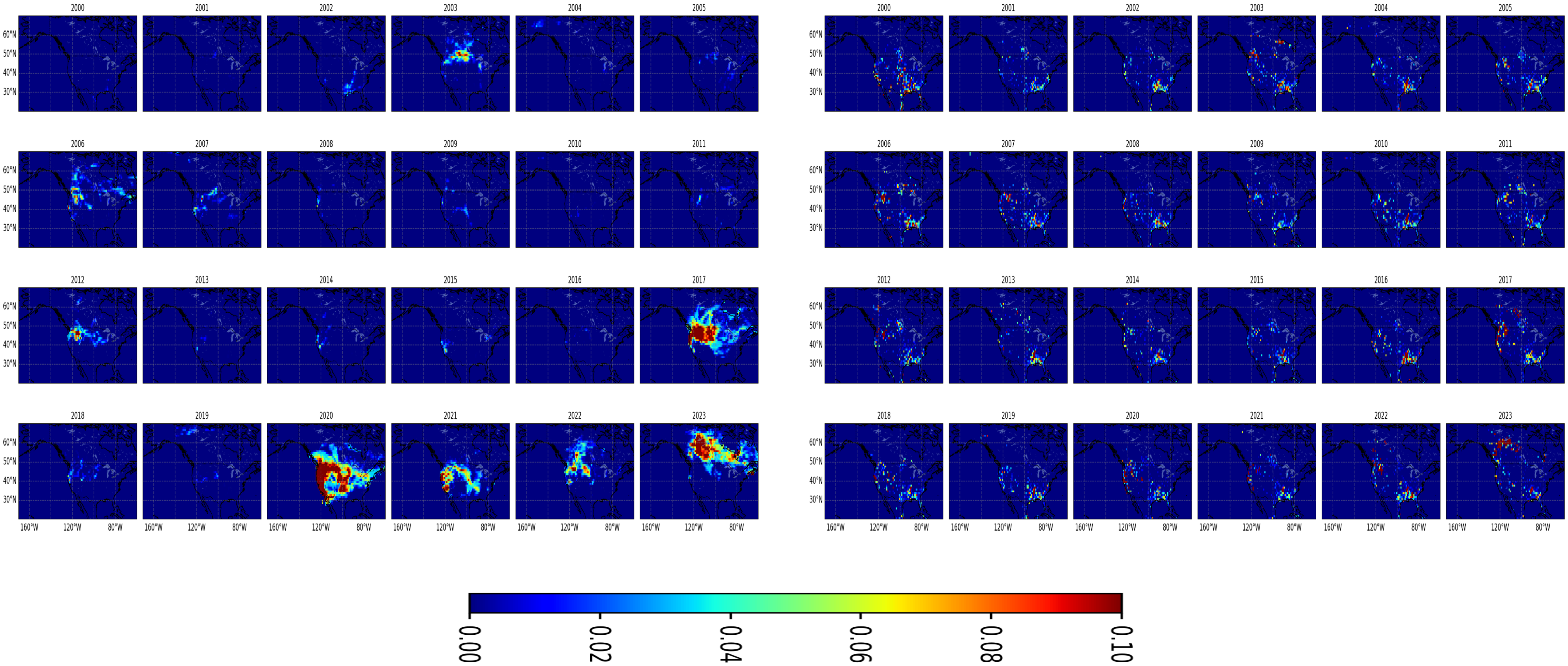

TIME SERIES

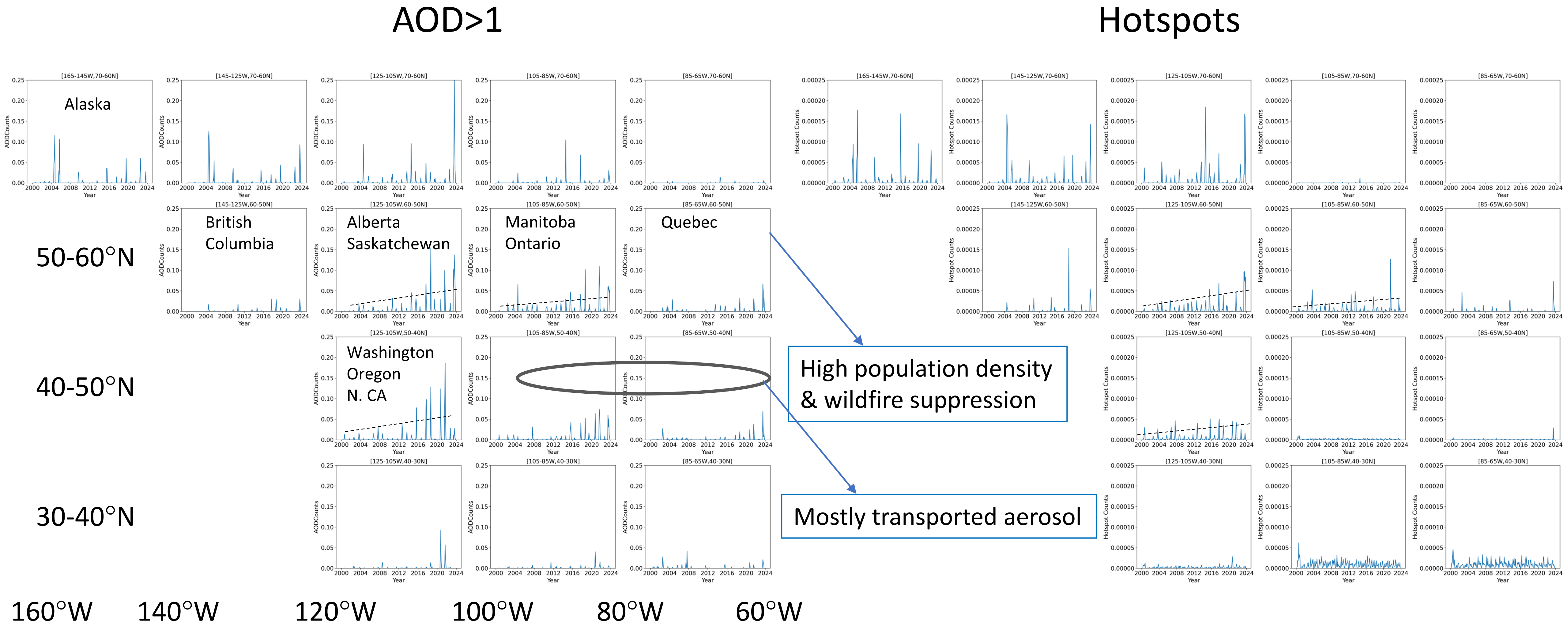

AOD>1
Hotspots
[165-145W,70-60N]
[145-125W,70-60N]
[125-105W,70-60N]
[105-85W,70-60N]
[85-65W,70-60N]
[145-125W,60-50N]
[125-105W,60-50N]
[105-85W,60-50N]
[85-65W,60-50N]
[125-105W,50-40N]
[105-85W,50-40N]
[85-65W,50-40N]
[125-105W,40-30N]
[105-85W,40-30N]
[85-65W,40-30N]
Alaska
British Columbia
Alberta Saskatchewan
Manitoba Ontario
Quebec
Washington Oregon N. CA
AODCounts
Hotspot Counts
Year
50-60°N
40-50°N
30-40°N
160°W
140°W
120°W
100°W
80°W
60°W
High population density & wildfire suppression
Mostly transported aerosol

Precipitation and Snow Fraction

February

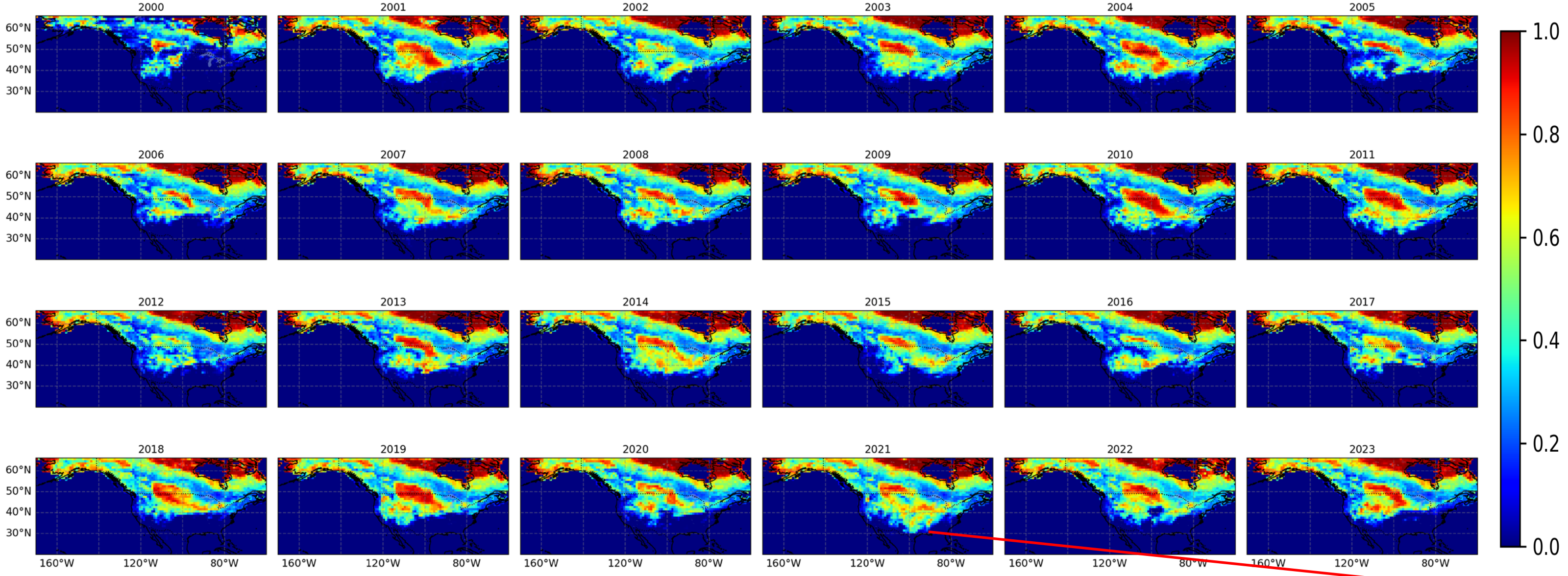

- Analysis of monthly precipitation, or precipitation accumulated in the past 2 to 4 months, did not show any correlation with fire, in agreement with Jain et al. (2022).

2021 Feb. Texas energy grid blackout

May

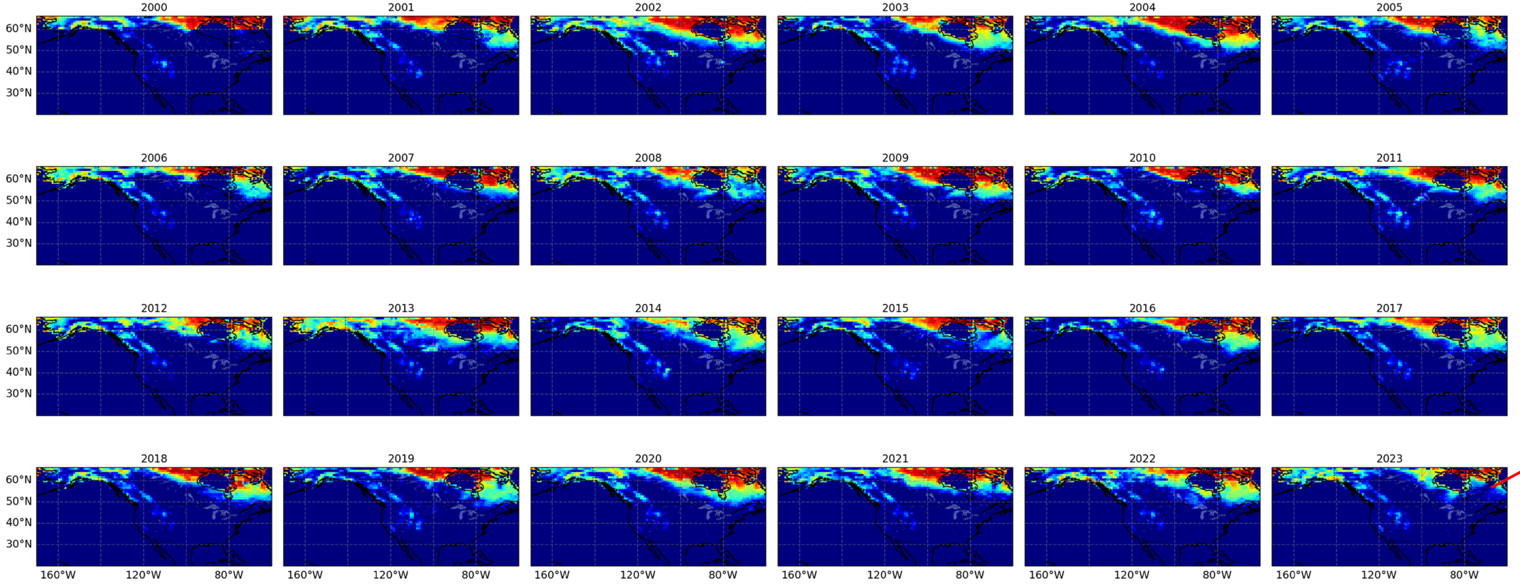

- No apparent correlation of SnowFrac with fire activity except possibly in North-East in 2023.

Anomaly Time Series

Snow Fraction

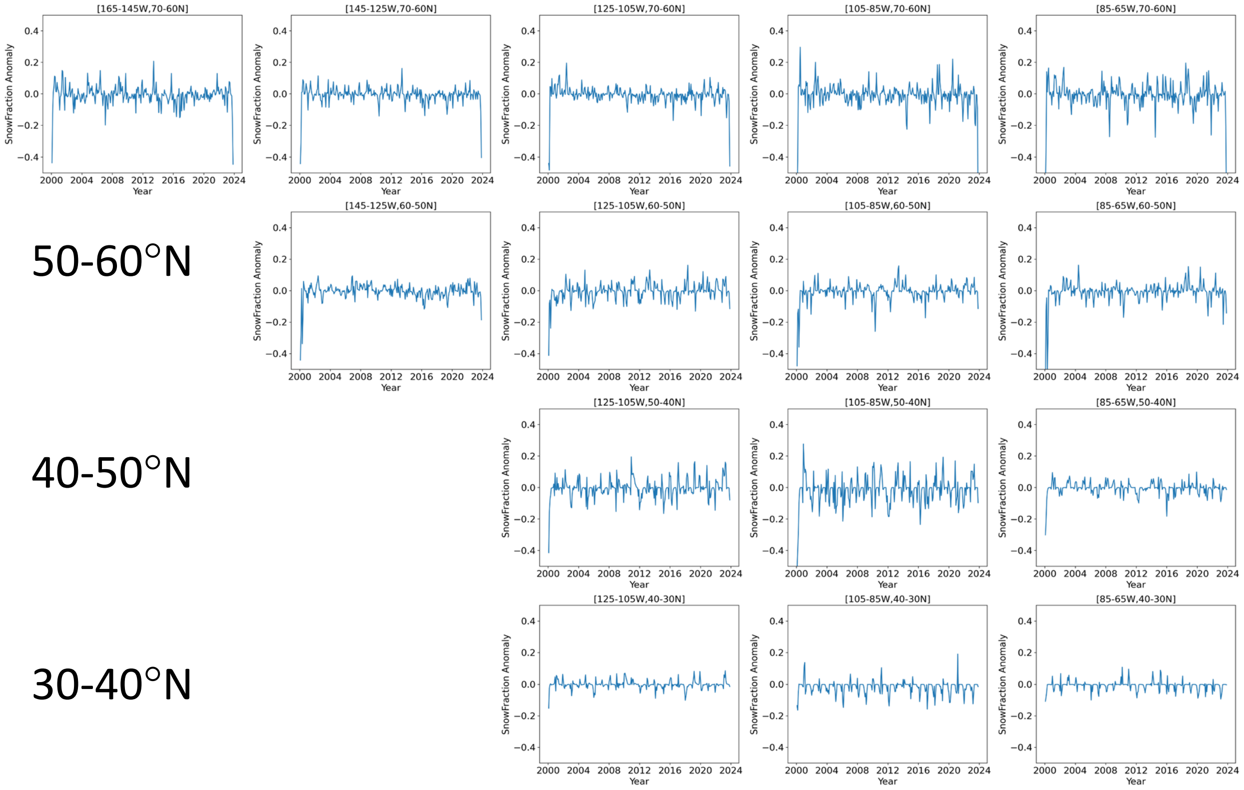

50-60°N

40-50°N

30-40°N

160°W 140°W 120°W 100°W 80°W 60°W

Precipitation (kg/m2/sec)

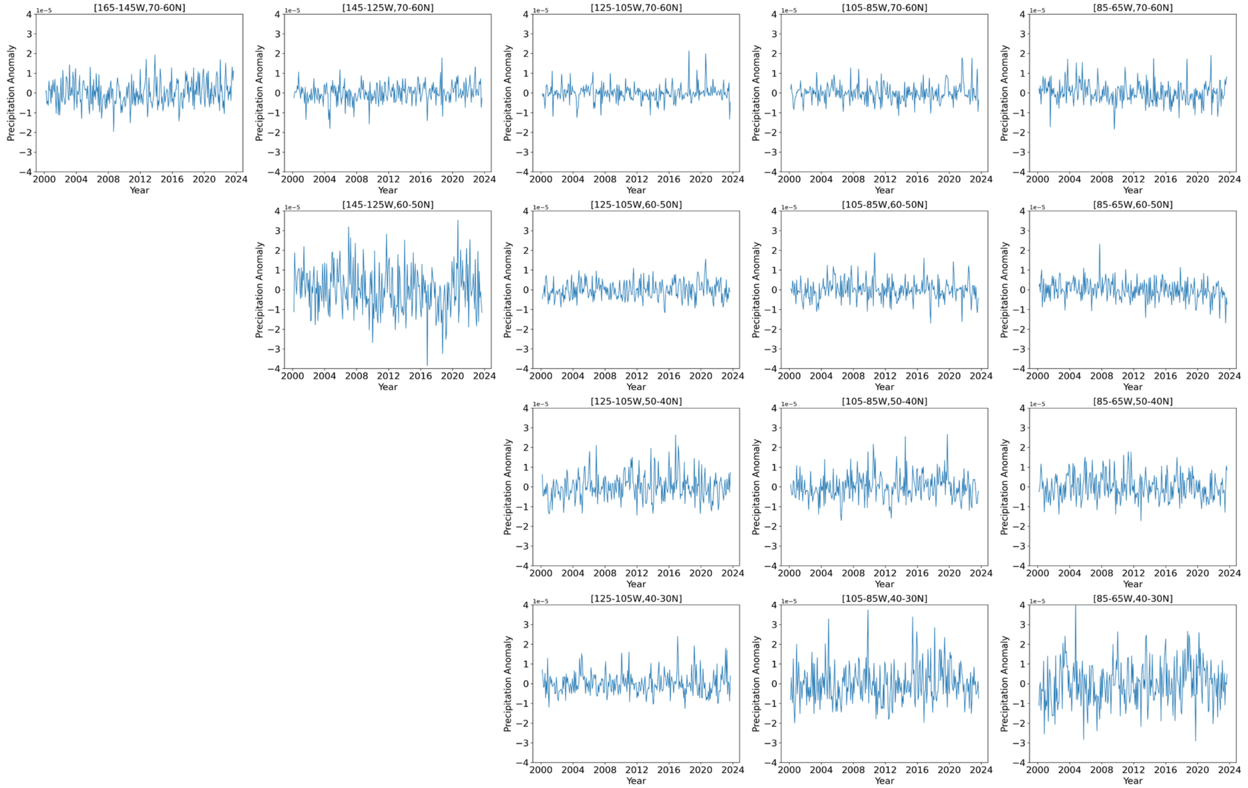

MAY

AOD>1

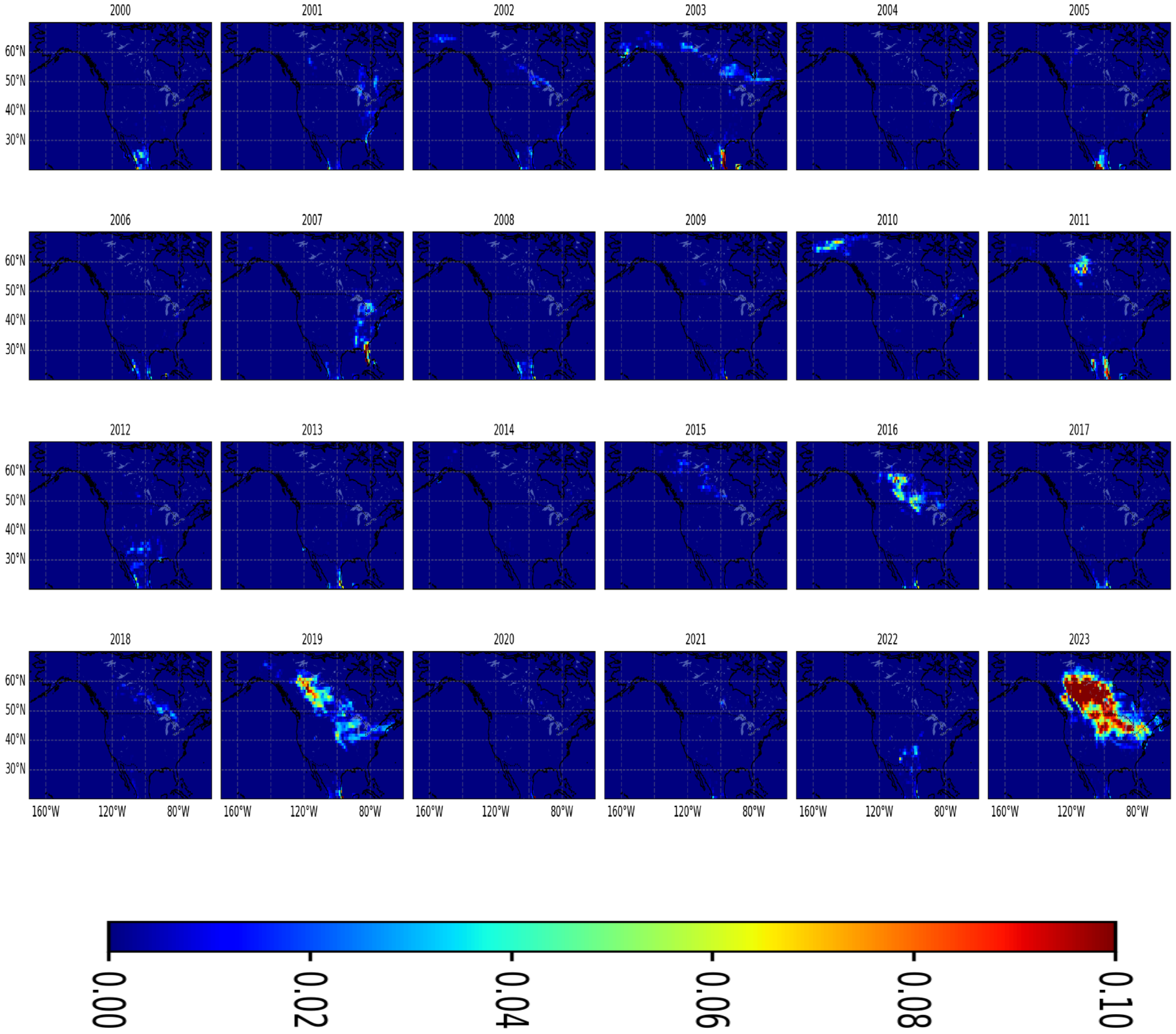

2m Air Temperature Anomaly, K

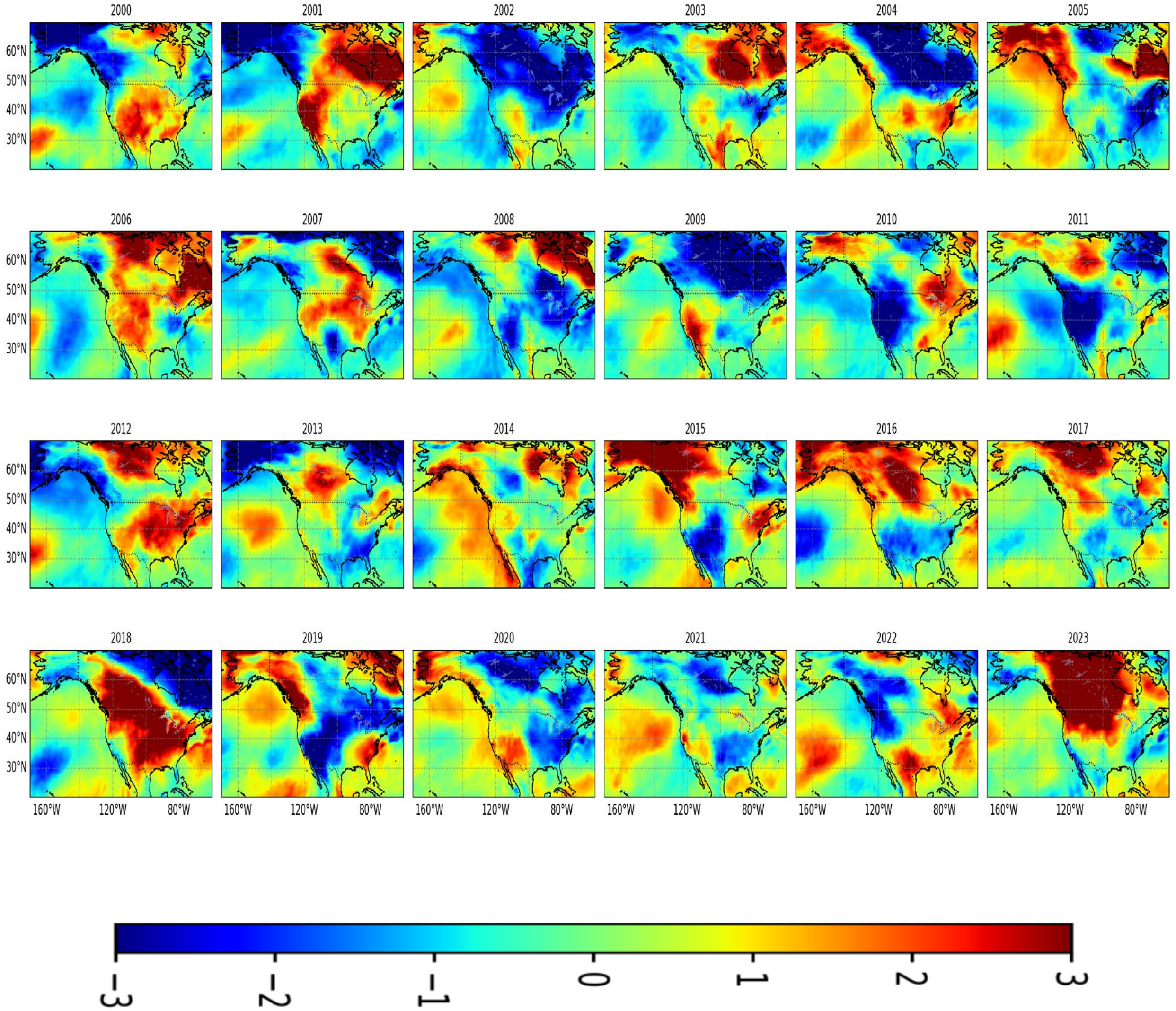

MAY

CWV Anomaly, cm

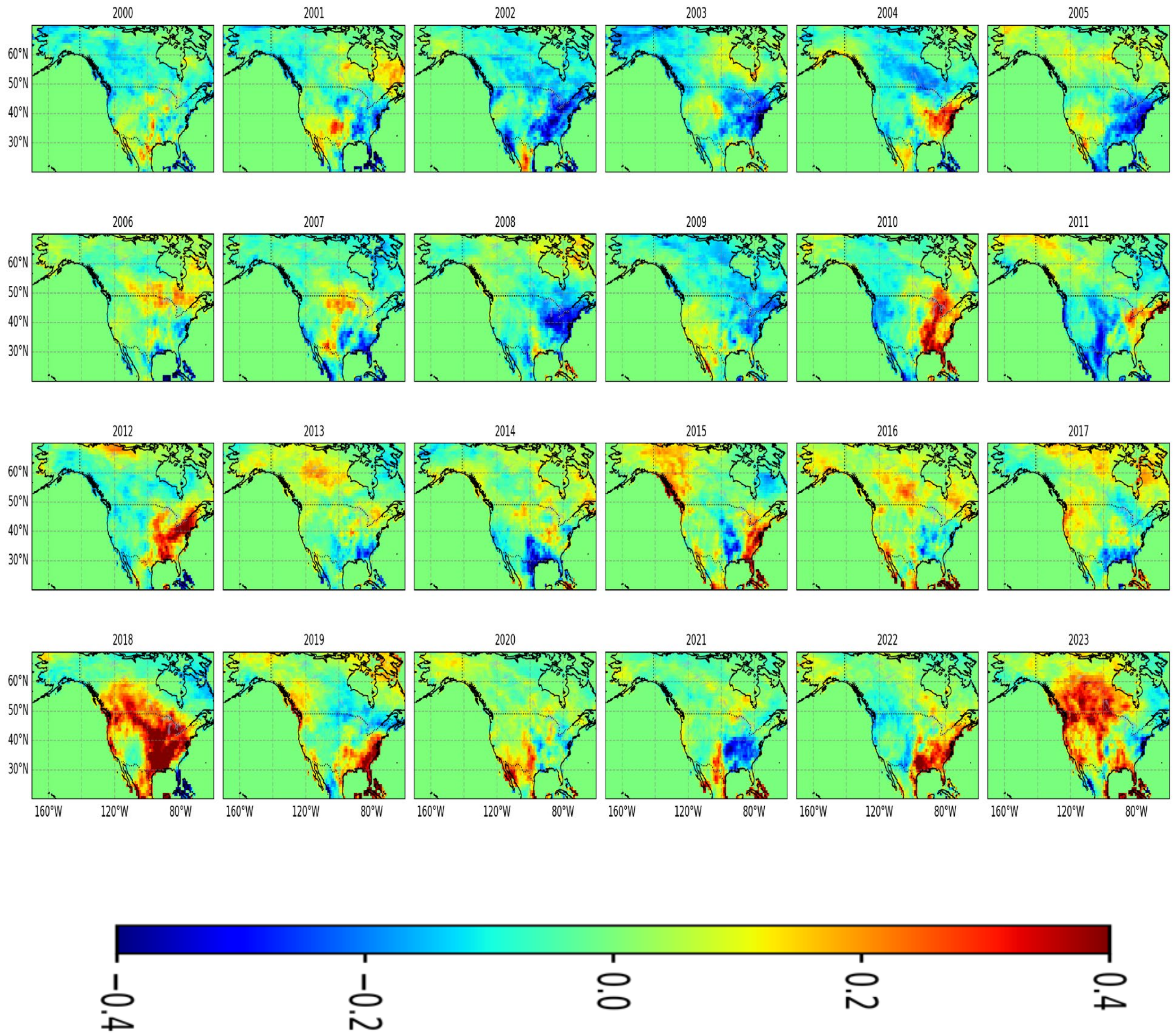

2m Air Temperature Anomaly, K

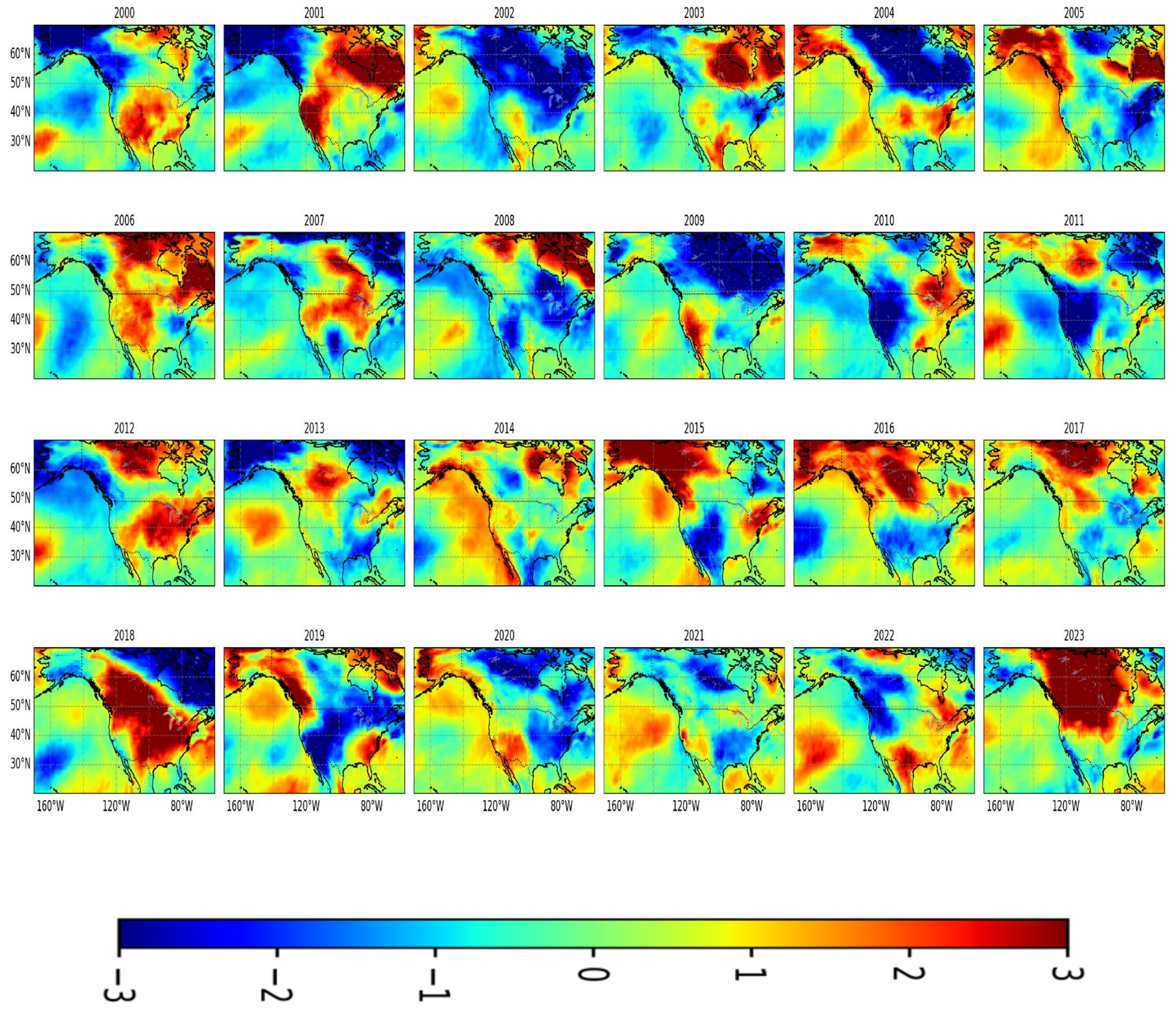

JUNE

AOD>1

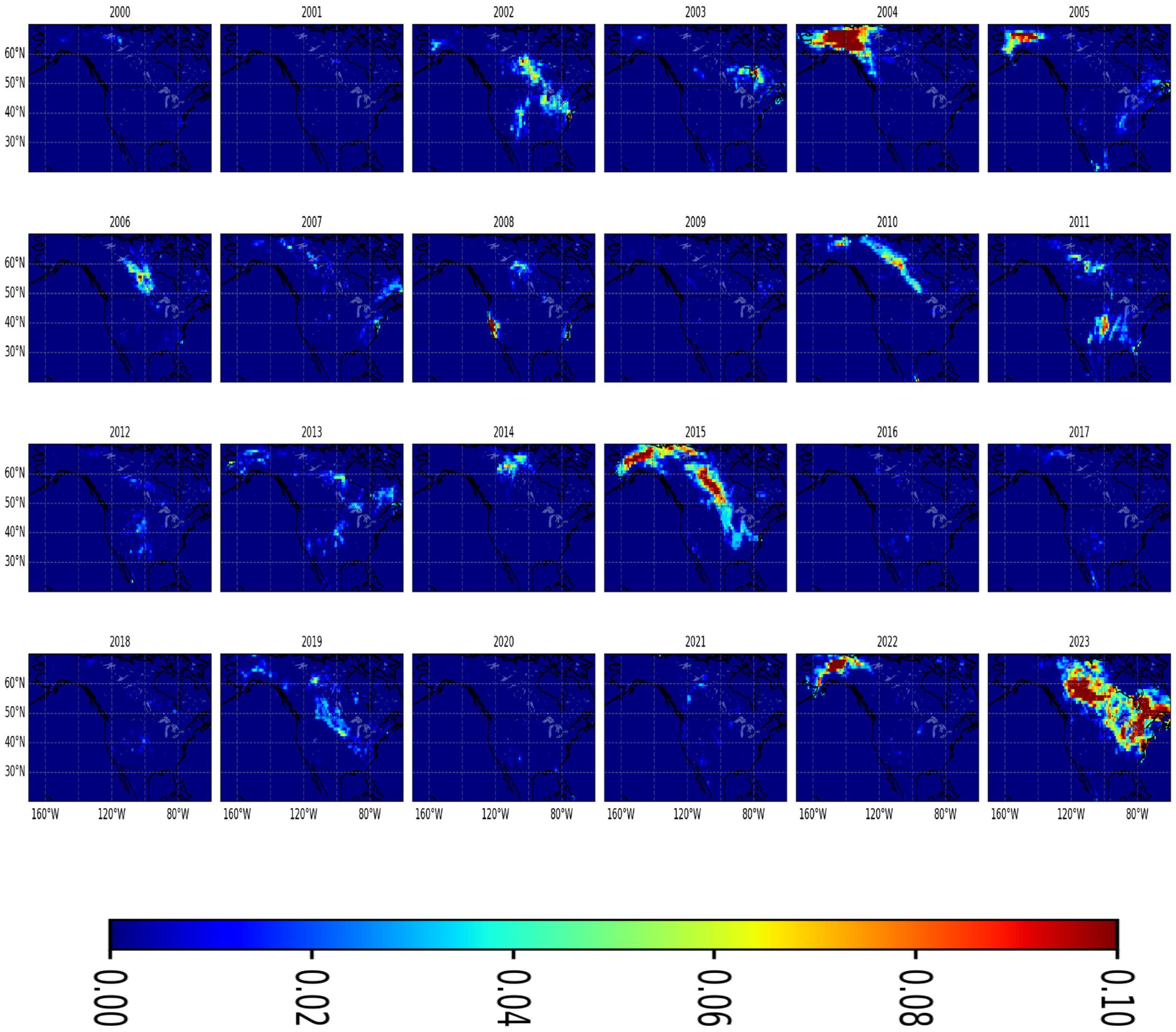

2m Air Temperature Anomaly, K

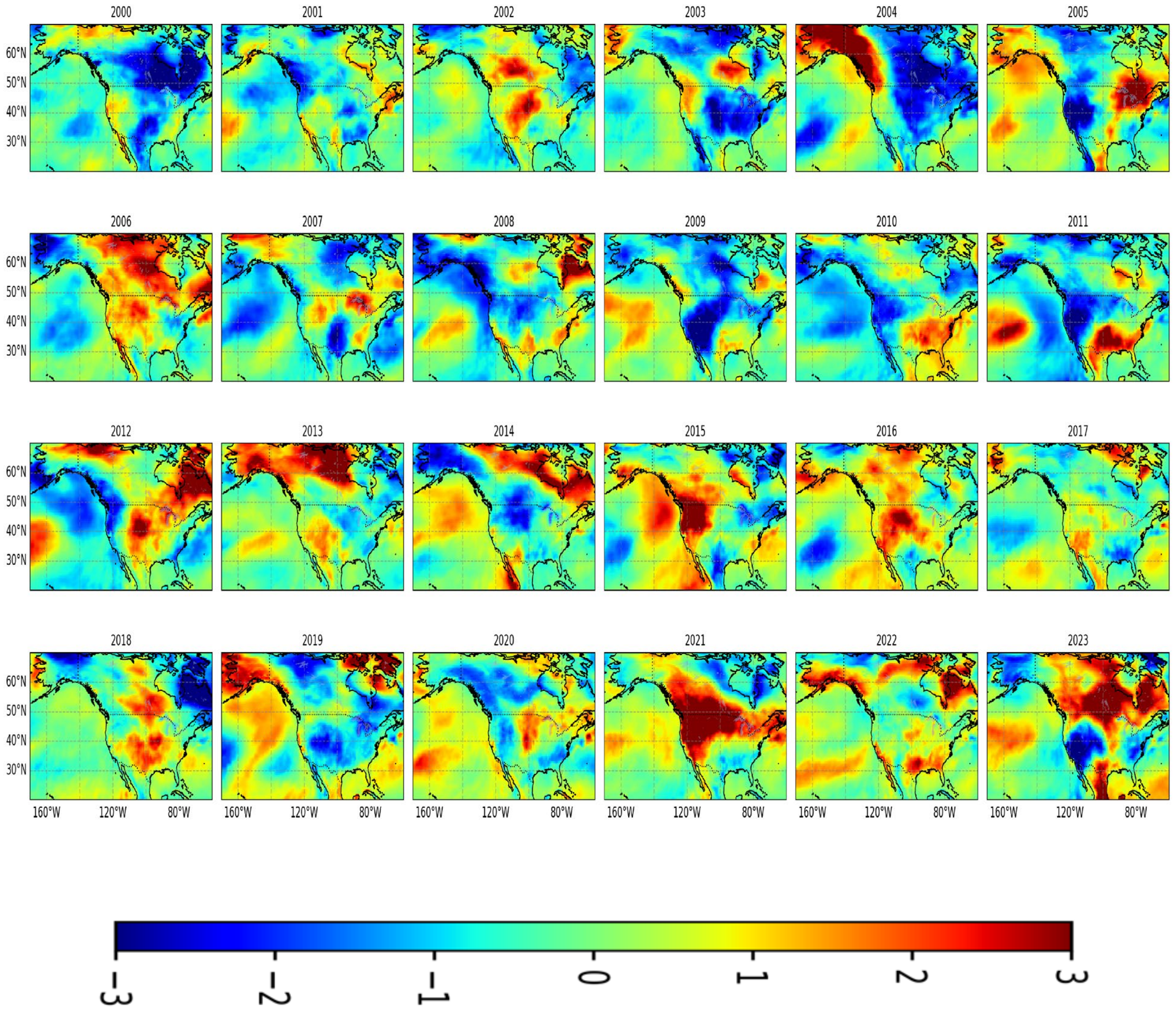

JUNE

CWV Anomaly, cm

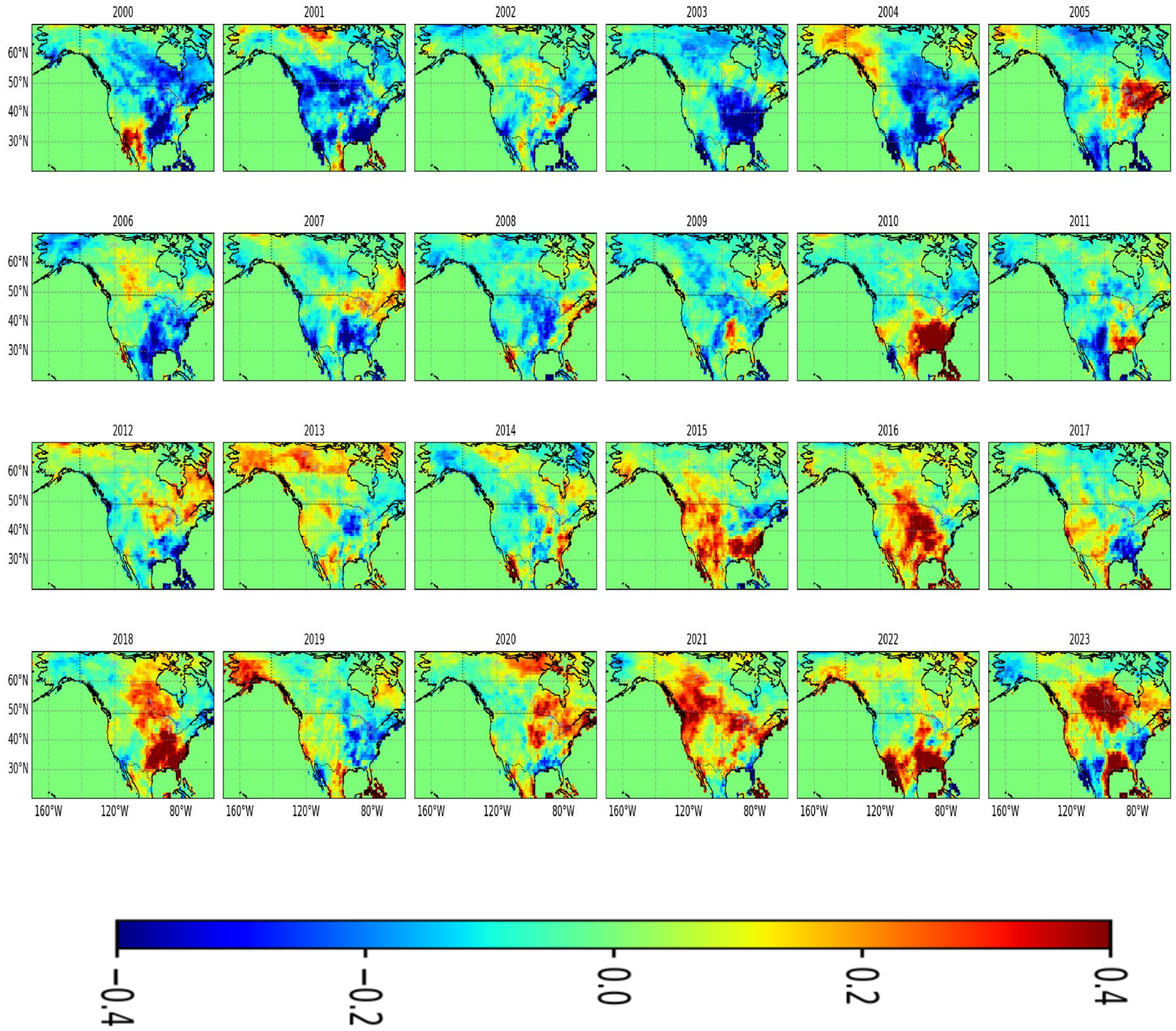

2m Air Temperature Anomaly, K

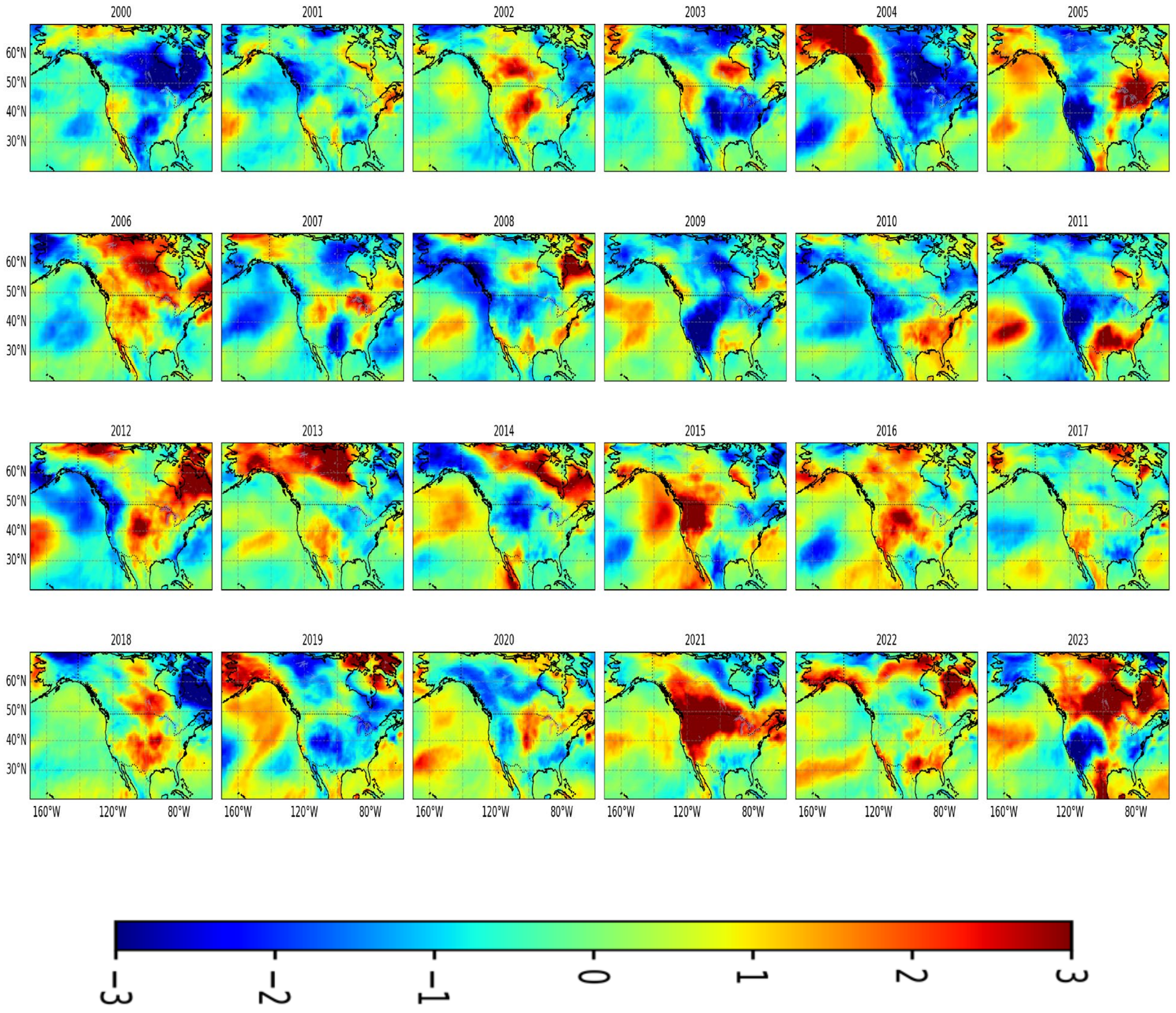

JULY

AOD>1

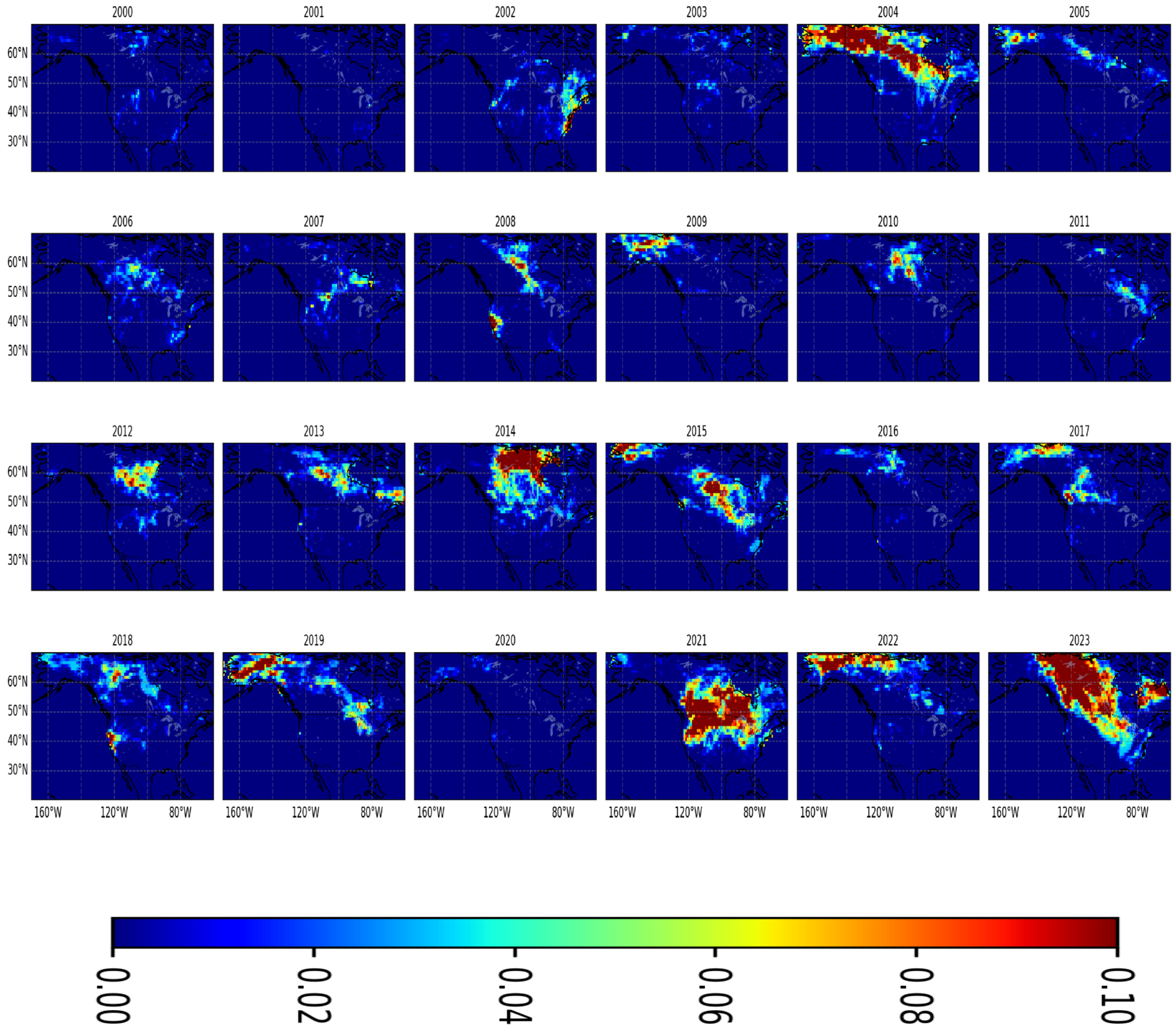

2m Air Temperature Anomaly, K

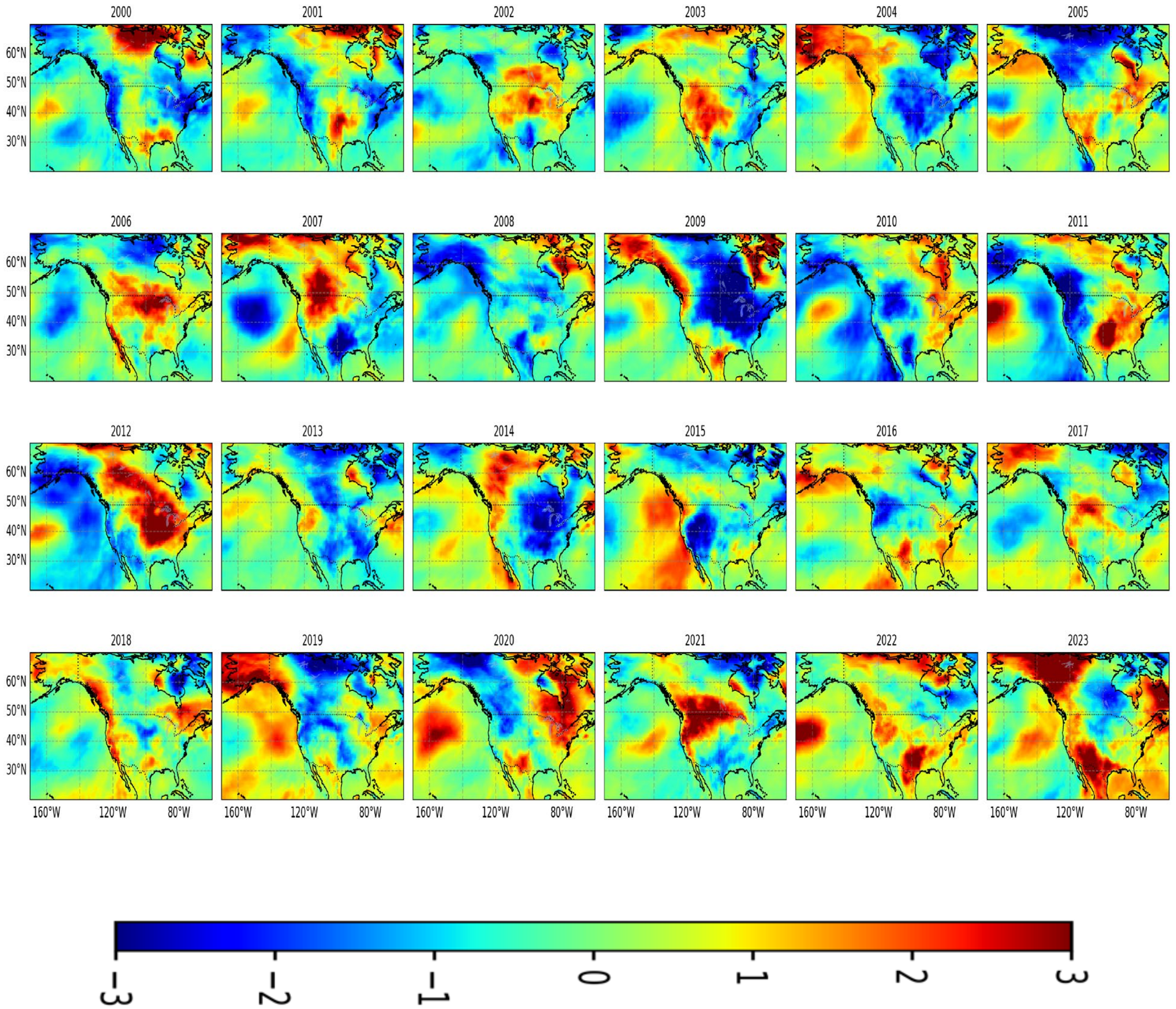

JULY

CWV Anomaly, cm

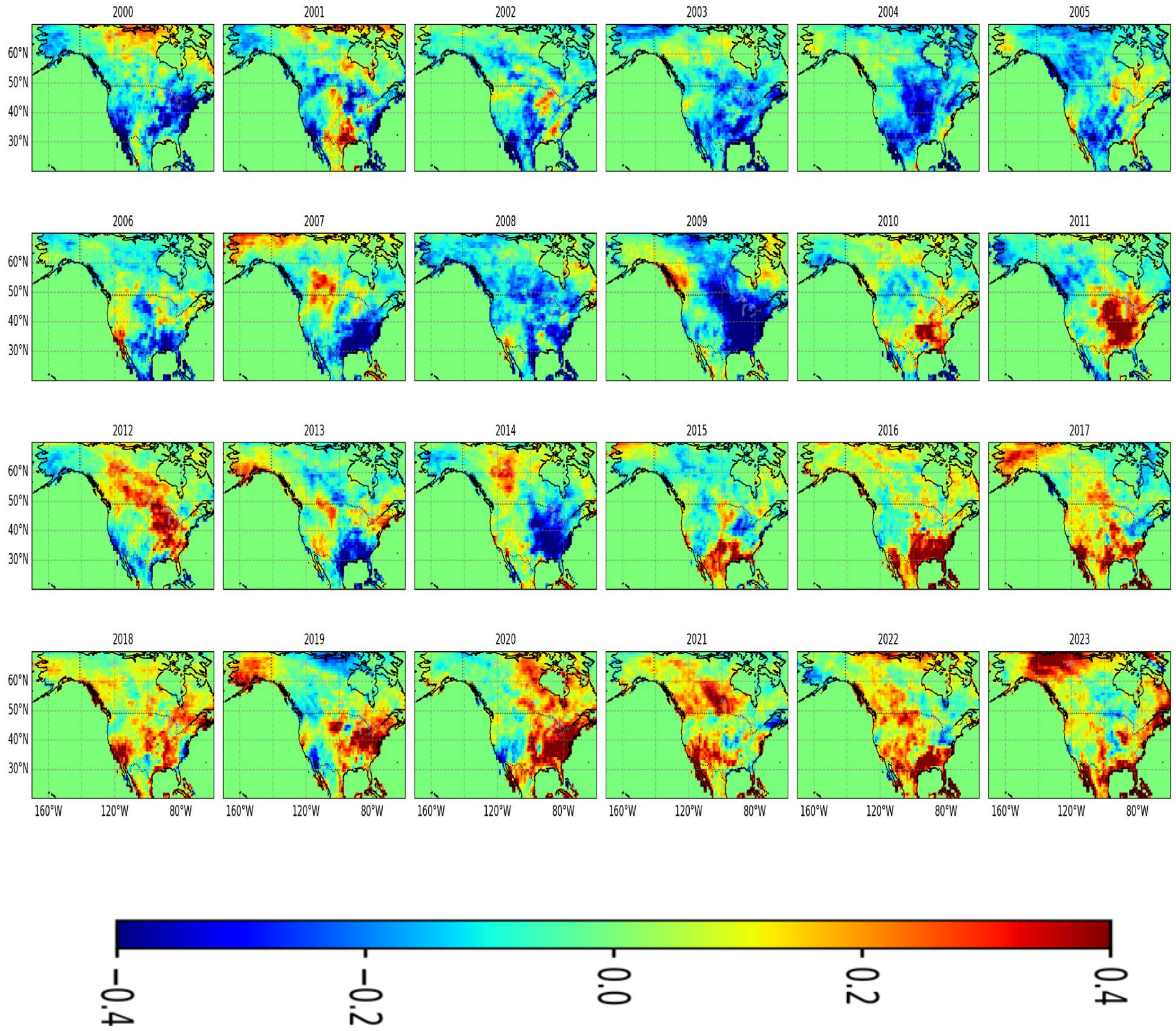

2m Air Temperature Anomaly, K

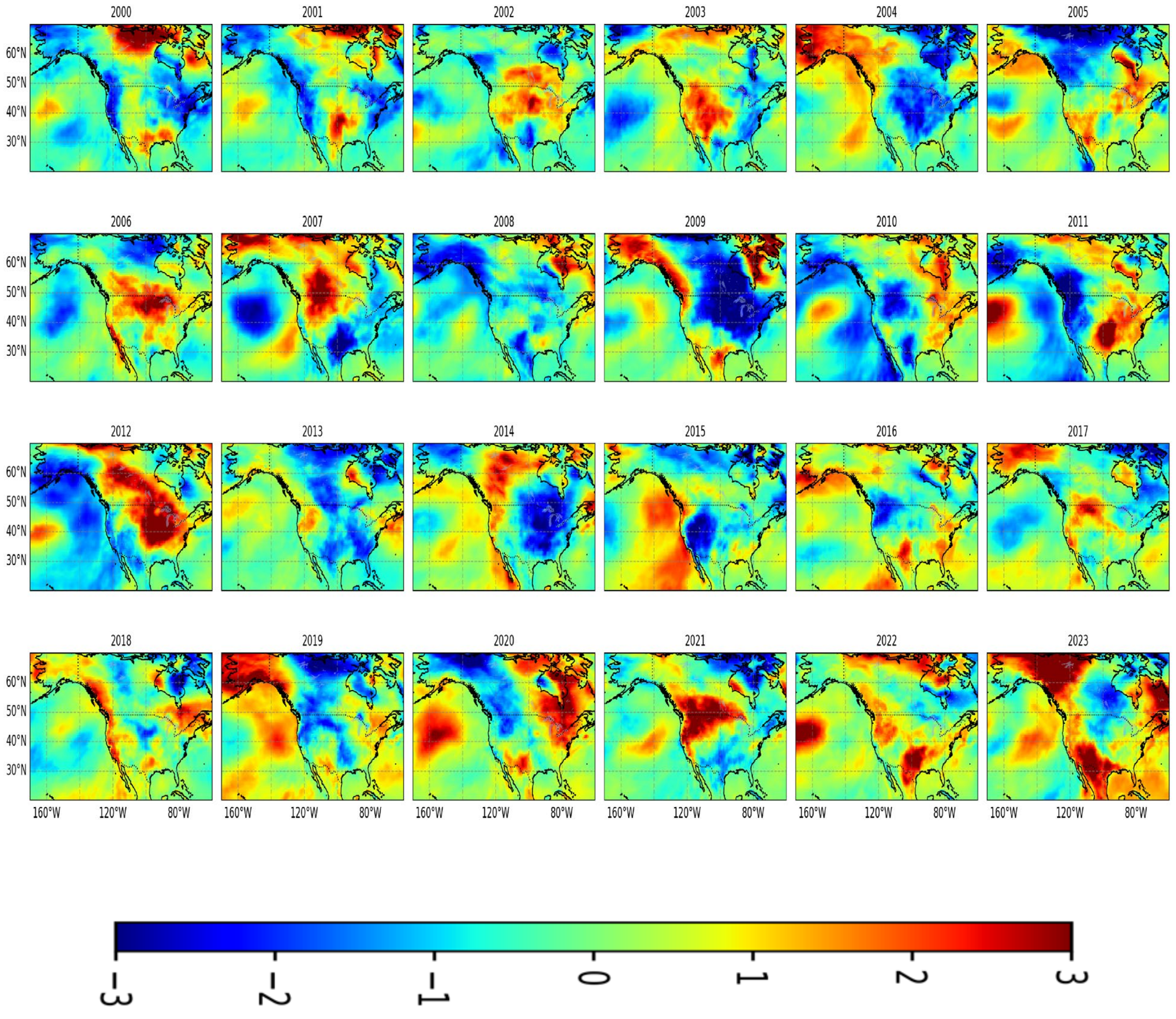

AUGUST

AOD>1

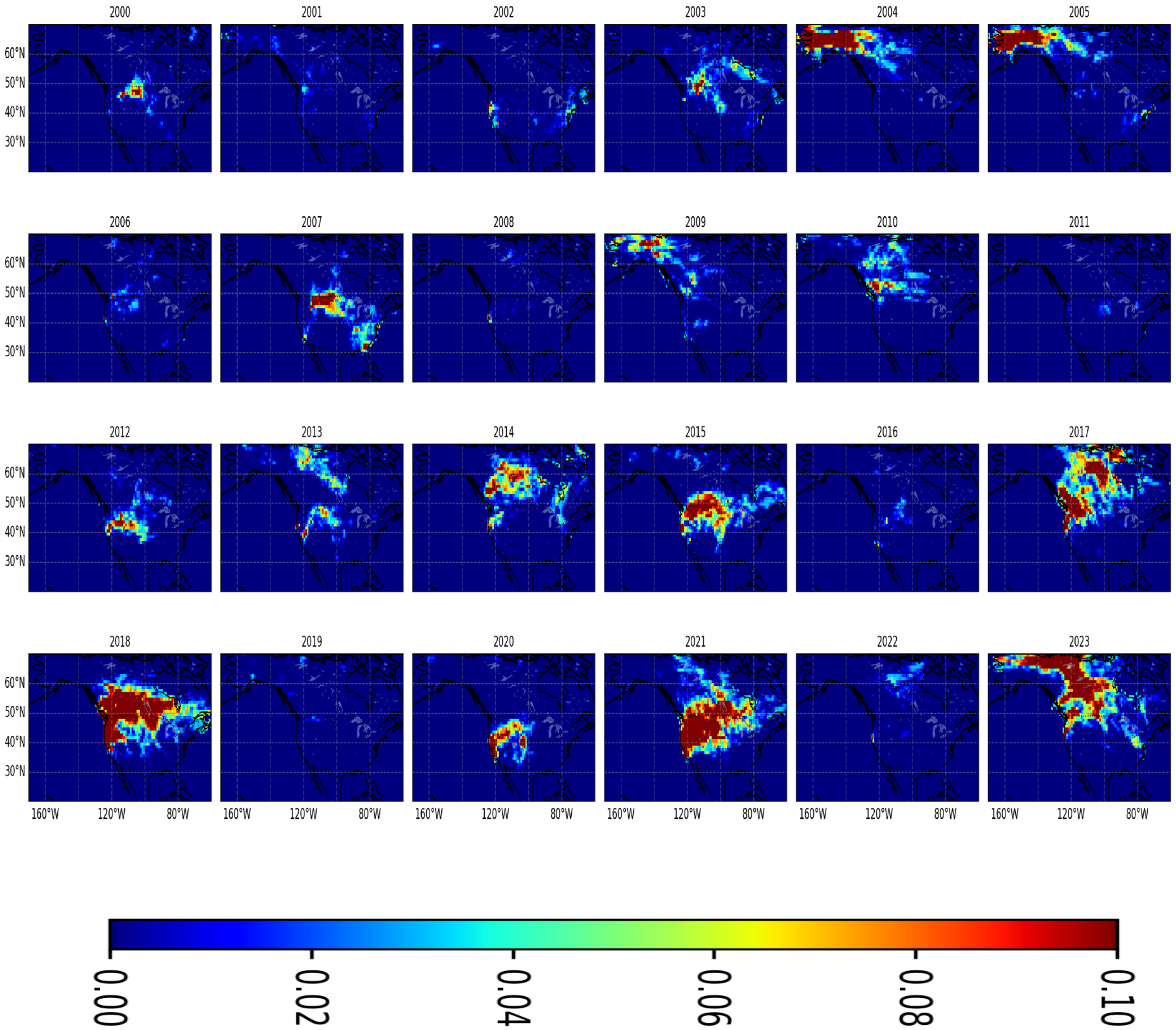

2m Air Temperature Anomaly, K

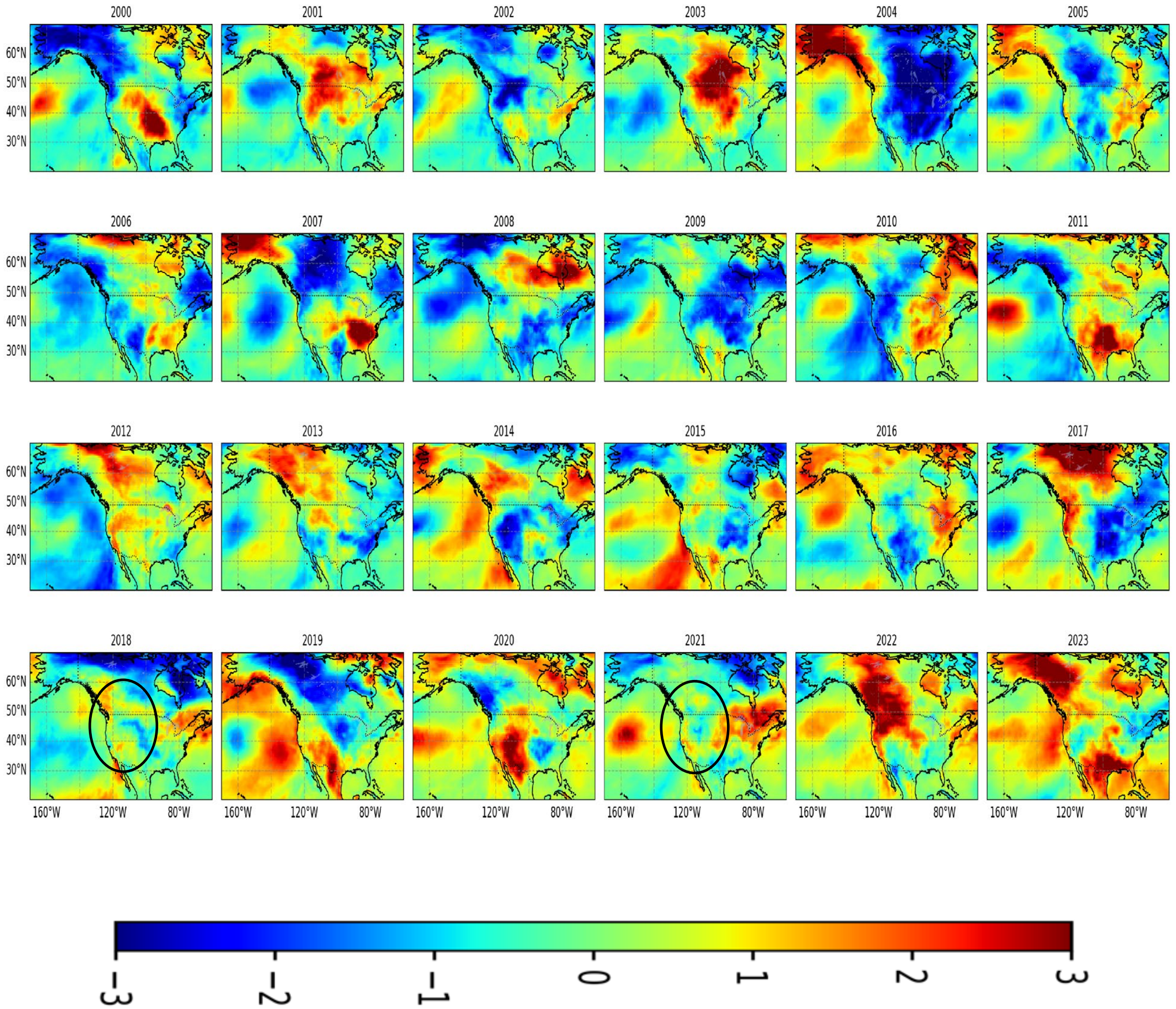

AUGUST

CWV Anomaly, cm

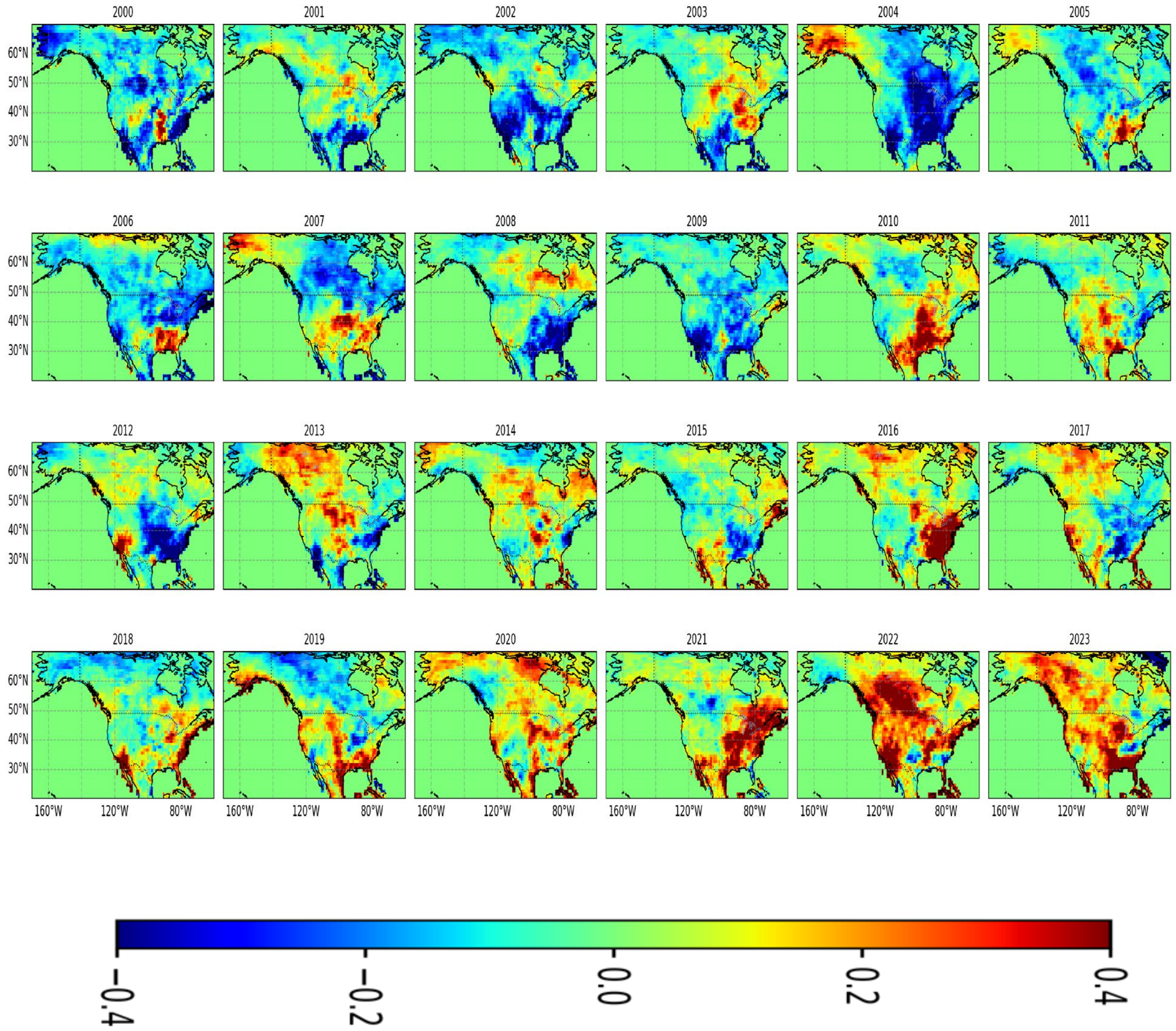

2m Air Temperature Anomaly, K

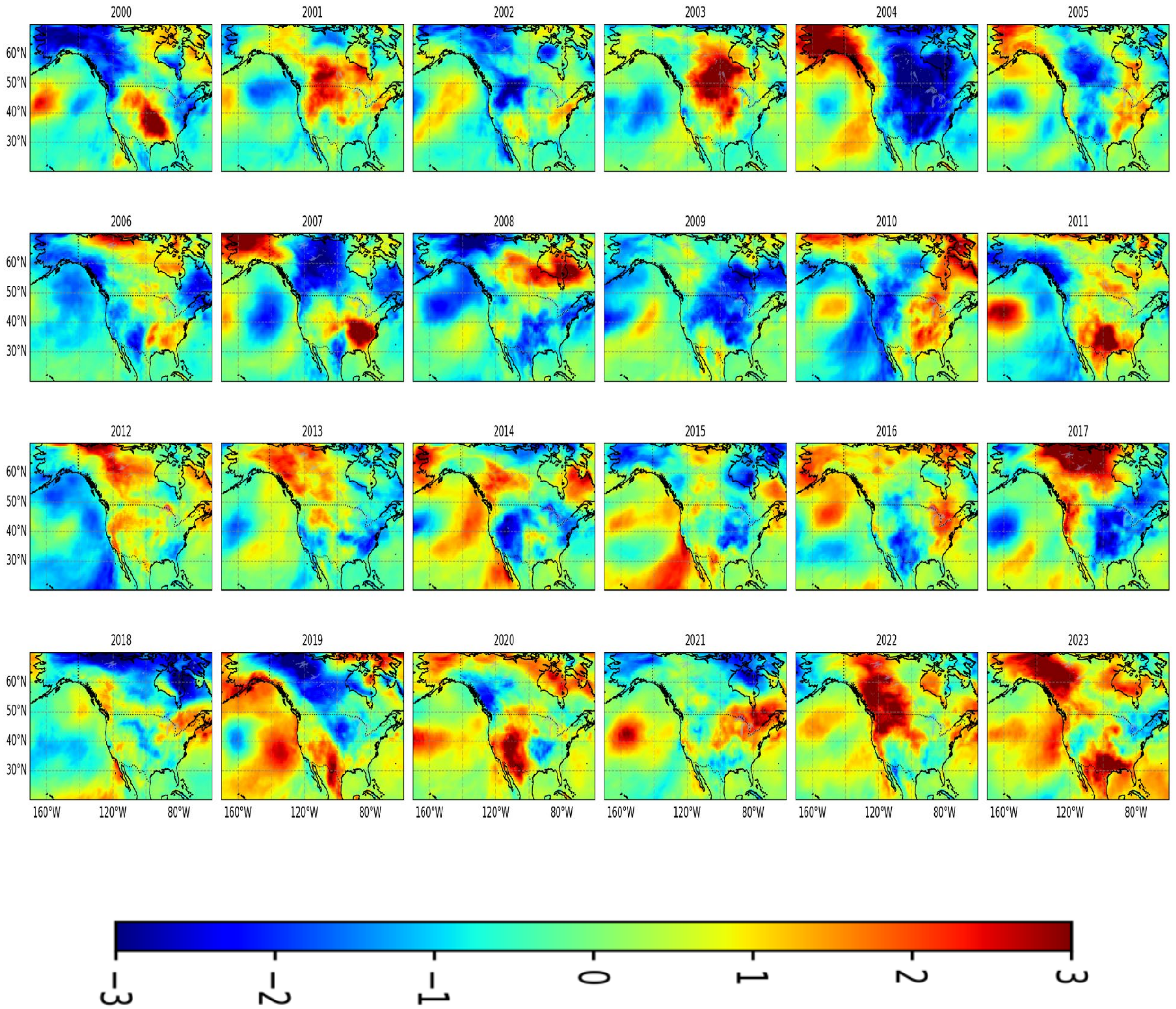

CONCLUSIONS

Analysis of ~24 yrs. (Feb. 2000 - Sept. 2023) of MODIS MAIAC record combined with MERRA-2 data over North America reveals:

- Significant trend in high AOD and fire hotspot (counts) at 50-60° in western and central Canada, and at 40-50° in north-western USA.
- We did not observe a link between fire activity and spring-time snow fraction from MAIAC, or precipitation (from monthly to lag-integrated for the past 2 to 4 months), in agreement with Jain et al. (NCom , 2022).
- From May through July, detected fires are correlated with positive temperature anomalies. This relationship may or may not hold for the rest of the fire season (August – September).
- From May through July, positive CWV anomalies are correlated with positive temperature anomalies (and fire activity) in fire-prone regions which is explained by abundance of moisture in soil/vegetation in spring-early summer.

Next, we plan to add analysis of MERRA-2 RH and computed VPD. A question is whether we can use anomalies in T-CWV (measurable by RS) to predict extreme fire weather.

fires-> high aerosol conditions. (Abatzoglou, J. T. and Williams, A. P.: Impact of anthropogenic climate change on wildfire across western US forests, *P. Natl. Acad. Sci. USA*, 113, 11770-11775, https://doi.org/10.1073/pnas.1607171113, 2016.)